73-24,841

PORTER, Jr., Hayden Samuel, 1945-
THE RESPONSE OF THE IONOSPHERIC F-LAYER TO ATMOSPHERIC GRAVITY WAVES AND ASSOCIATED AIRGLOW PHENOMENA.

University of Cincinnati, Ph.D., 1973
Geophysics

University Microfilms, A XEROX Company, Ann Arbor, Michigan

THE RESPONSE OF THE IONOSPHERIC F-LAYER TO ATMOSPHERIC GRAVITY WAVES AND ASSOCIATED AIRGLOW PHENOMENA

A dissertation submitted to the

Division of Graduate Studies
of the University of Cincinnati

in partial fulfillment of the
requirements for the degree of

DOCTOR OF PHILOSOPHY

in the Department of Physics
of the Graduate School of Arts and Sciences

1973

BY

Hayden Samuel Porter, Jr.

B.S. University of Cincinnati, 1967

UNIVERSITY OF CINCINNATI

May 16 *19* 73

I hereby recommend that the thesis prepared under my supervision by Hayden S. Porter, Jr.

entitled The Response of the Ionospheric F-Layer To Atmospheric Gravity Waves and Associated Airglow Phenomena

be accepted as fulfilling this part of the requirements for the degree of Doctor of Philosophy

Approved by:

Form 668—Grad. School—1M—3-69

ABSTRACT

We develop a fully time dependent analytical treatment of F-layer response to disturbances arrising either through momentum transfer from the neutral constituents or through ion pair production or loss mechanisms. The ion equation of motion, including an ion drag term, and the ion continuity equation, including a linear loss term and an arbitrary ion pair production term, are solved simultaneously using Green's function and integral equation methods. It is assumed that typical horizontal scales for variations in the disturbance are large in comparison to the vertical half width of the F-layer, so that a description using only one spatial dimension is applicable. It is also assumed that the disturbance is sufficiently slowly varying in time that quasistatic equilibrium holds in the ion equation of motion. The treatment includes diffusion, and the linear loss term contains an arbitrary scale height factor p which allows the atmospheric state to vary from perfect mixing (p=1) to diffusive equilibrium (p=2).

The treatment is applied to calculating the response of the F-layer to passage of atmospheric gravity waves. In this approach, unlike other approaches where perturbation methods are applied, the undisturbed F-layer is itself time dependent. This treatment can be used for disturbances sufficiently large that a strict perturbation approach can no longer apply.

A simple gravity wave model is chosen which allows the velocity amplitude to be varied from constant with altitude to various degrees of exponential increase. The time dependence is assumed to be sinusoidal. Analytical solutions obtained using this model are compared with Thome's detailed experimental study of the ionospheric response to gravity waves. The theoretical results agree well with the following observed experimental features: 1) Normalized time dependent electron density fluctuations at constant altitude, 2) root mean square oscillation amplitude as a function of altitude, 3) changes in phase of the oscillation as a function of altitude, and 4) time variations of hmF2.

Several interesting features of the ionospheric response are found. The F-layer response to sinusoidal gravity waves is not in general sinusoidal or even periodic. The F-layer response to gravity waves dies away as the F-layer decays even though the gravity wave itself continues unattenuated. Fluctuations in the electron density at about two scale heights below the F-layer peak are typically 6 to 8 times larger than fluctuations at the peak. The amplitude of the normalized electron density fluctuation goes asymptotically to a constant value for high altitudes and this value depends upon the degree of the exponential growth exhibited by the wave.

The effect of gravity waves on the 6300Å OI and 5200Å NI airglow emissions excited via dissociative recombination is also studied. It is found that relatively large percentage fluctuations may occur both in the the magnitude of the peak of the luminosity profiles and in the zenith airglow intensity. The amplitude of fluctuation depends upon the gravity wave velocity amplitude as well as the altitude at which the peak of the luminosity profile occurs. Since variations in the quenching rates may appreciably change the altitude of the peak of the luminosity profiles, the fluctuation amplitude of the zenith airglow intensity is sensitive to variations in the quenching rate. Zenith airglow intensity fluctuations in the 6300Å OI line of the order of 15% are found for the parameters used in the fit to Thome's experiment. A comparison of our theoretical fit to the 6300Å airglow measurements obtained by Dachs shows good agreement in the h'F2, f_oF2 and zenith airglow intensity. The fluctuation amplitude of the 5200Å NI line is found to be sensitive to the quenching rate with O_2 relative to that with electrons. An increase in the electron quenching rate, for example, effectively translates the 5200Å NI luminosity profile lower in altitude and consequently increases the fluctuation amplitude of the zenith airglow intensity.

ACKNOWLEDGEMENTS

I am pleased to acknowledge the following individuals and organizations for their assistance in the completion of this dissertation.

It is with the greatest pleasure that I express my gratitude to Professor Tai-Fu Tuan both for his suggestion of this problem and for his continued assistance and guidance.

I am grateful to Professors Bernard Goodman, Ernst Franke, and Marion Gunther for serving as committee members and to Professor Dale Jones for demonstrating continued interest.

I wish to thank Dr. Sam Silverman for several stimulating discussions concerning this problem.

I also wish to express my appreciation to Dr. George Thome for making available the unpublished electron density profiles.

I am indebted to the Air Force Cambridge Research Laboratories Contract AF 19628-71C-0028-P00001, the National Atmospheric amd Space Administration, and the University of Cincinnati for their financial assistance.

Finally, I wish to thank my wife Pat, not only for the typing of this dissertation, but also for her continued efforts to provide a pleasant atmosphere in which to work.

TABLE OF CONTENTS

LIST OF TABLES

LIST OF ILLUSTRATIONS

Chapter 1

Introduction

The phenomena of traveling ionospheric disturbance (TID) has received a rather large amount of attention over the last several years. Observations of the ionosphere have demonstrated that TID is a relatively common occurrence. Generation mechanisms for TID advanced have included nuclear blasts, magnetic substorms, and the breakdown of large scale tidal motions in the atmosphere. Evidence of TID can often be observed on critical frequency plots. TID appears as quasi-periodic ripples which are superimposed on the normal diurnal behavior. In certain cases characteristic peaks or troughs noted in the critical frequency plots obtained at one ionospheric observatory can be identified in the critical frequency plots obtained for other observatories which are widely spaced in both latitude and longitude. This occurrence suggests that TID is propagated over large distances. Analysis by Bowman (1965) even suggests that some waves are capable of propagating entirely around the earth. Perhaps the most salient feature of TID is that vertical variations invariably show a downward component of motion. This apparent motion can be interpreted as a downward phase progression; however, it is recognized that this motion can also be attributed to an inclined front moving horizontally.

The principal mechanisms advanced to explain TID are hydromagnetic waves propagating through the ionized gas and compressional waves propagating through the neutral atmosphere. The first author to attempt theoretical explanation of TID was Martyn (1950). Martyn solved the linearized fluid equations of the neutral atmosphere under the influence of gravity. Assuming the existence of two well defined horizontal boundary layers, he obtained solutions corresponding to horizontally traveling convection cells in the neutral atmosphere. Martyn reasoned that these motions of the neutral constituents could produce, via collisions, oscillations in the ionized species similar to those observed in TID. The success of this model was limited, however, largely because it required the existence of a horizontal boundary layer at, or near the altitude of the F-layer peak.

Interpretation of TID in terms of hydromagnetic waves was suggested by Dungey (1955) and Akasofu (1956). In this interpretation hydromagnetic waves were generated either by processes occurring in the outer regions of the atmosphere or in the solar corona, and were propagated down into the lower regions of the atmosphere through the ionized gas. The attractiveness of this model was its ability to explain the downward progression of the disturbance; however, typical Alfven velocities for the F-layer were much larger (~2000 m/s) than the observed TID velocities (~150 - 700 m/s).

The currently accepted interpretation of TID was advanced by Hines (1960). Hines obtained internal wave solutions for the neutral atmosphere under the influence of gravity. These solutions were found to form two branches, termed the acoustic and gravity wave branches. The acoustic wave branch corresponds to a generalization of normal sound waves to include gravitational effects. The gravity wave branch was distinguished by its long period of oscillations which must be greater than the local Brunt-Väisälä period (about 14 minutes in the F-layer). Certain properties of the gravity wave branch solutions, such as the long period, correct range of permitted phase velocities, and exponential growth with altitude, strongly suggested a connection with TID. Hines (1960) suggested as did Martyn (1950) that these motions of the neutral constituents could produce, via collision, oscillations in the ionized constituents similar to those observed in TID.

It is the effect of these internal gravity waves on the ionosphere and on associated airglow phenomona which we investigate in this dissertation. Specifically, we develop an analytical time dependent treatment of F-layer response, including effects of momentum transfer from the neutral species and arbitrary ion pair production or loss mechanisms. This treatment is limited to disturbances for which approximate quasistatic equilibrium holds in the ion equation of motion. Horizontal variations in the disturbance are assumed to be slowly varying over distances large compared to the vertical thickness of the F-layer, so that a model requiring only one spatial dimension may be used. A neutral wave model is chosen which allows full use of the analytical features of this treatment. We develop solutions for long period, long wavelength, ducted internal waves. A solution obtained using this model is compared with the detailed experimental observation of TID at Arecibo by Thome (1968). We also consider gravity wave induced behavior in the volume emissivity and integrated airglow intensity for both 6300Å OI and 5200Å NI. Comparisons between our theoretical results and Dachs (1968) 6300Å airglow intensity measurements are made.

Analytic solutions to F-layer problems have been developed by many workers. Ferraro (1945, 1946) discussed the importance of the diffusion of ions in the F-layer and set forth the mathematical apparatus for plasma diffusion. Ferraro and Ozdogan (1958) obtained solutions to the diffusion equation of the ionized constituents for a periodic production function representing the production of ion pairs by extreme ultraviolet solar radiations. The recombination of ion pairs was approximated by a loss term which was linear in the electron density. The recombination coefficient was altitude independent.

Glidden (1959b) solved the problem posed by Ferraro and Ozdogan (loc. cit.) for a recombination coefficient which varied with altitude according to the scale height of the major neutral constituent. This choice of recombination coefficient is equivalent to the assumption of perfect mixing of the atmospheric constituents. Using perturbation methods, Tuan (1968) treated the problem of the night-time behavior of the F-layer when the altitude dependence of the recombination coefficient is governed by an arbitrary scale-height factor p. In this model p=1 corresponds to perfect mixing of the atmospheric constituents, while p=2 corresponds to diffusive equilibrium. Moschandreas and Tuan (1973), using Green's function and integral equation methods, treated the problem of an arbitrary production or loss mechanism and arbitrary scale-height factor.

Within the framework of F-layer theory there have been many attempts addressed to the development of a description of F-layer response to internal gravity waves. The nature of these attempts has been to demonstrate that the behavior of the F-layer when perturbed by internal gravity waves exhibits essentially the same characteristics as exhibited by TID. Perhaps somewhat surprisingly, however, the general trend of these treatments has been to use a perturbation approach similar to that used in a discussion of the neutral waves, rather than follow the established line of F-layer theory. In the perturbation approach it is assumed that the ionized parameters can be written as a time independent part plus some small time dependent correction due to the gravity wave. While this assumption is certainly reasonable for the neutral constituent where production and recombination processes are not important, it is not clear that it is a reasonable assumption for the ionized species. For example, it is often found that the period of a TID is approximately the same as the mean decay time of the F-layer. Thus, if the ion pair production rate is small the assumption that the unperturbed ionosphere is time independent is certainly not valid.

While a fully consistent solution to this problem requires simultaneous solution of the coupled neutral and ion equations, most authors are primarily concerned with the ionospheric response and solve the ion equations independently, assuming some model for the neutral wave. The first quantitative treatments of the response of the F-layer to gravity waves appeared in 1968. Hooke (1968) used perturbation methods as discussed above. Although developing the response calculations fully, he eventually neglected effects of diffusion, as well as production and loss of ion pairs. To obtain his final solution he makes the additional assumption that the ionospheric response at a given altitude to a sinusiodal gravity wave is sinusoidal. Results of this calculation show the existence of a phase change in the oscillation. The altitude of this phase change is time independent but does depend on the degree of exponential growth of the neutral wave.

Using the method of characteristics, Nelson, (1968) obtained analytic solutions of the ion continuity equation for certain choices of the neutral wave model. These solutions are obtained under the assumptions that diffusion can be neglected and that production and loss processes are exactly balanced. The essential feature of this approach is that the time dependent behavior of the F-layer is obtained from solution and not assumed. Results of this treatment show the existence of a phase change in the oscillation. The altitude at which this phase change occurs is time dependent and also depends on the degree of exponential growth of the neutral wave. Unfortunately, the assumptions are such that the results can not be directly applied to existing TID observations.

Testud and Francois (1971), using perturbation methods have obtained solution to the ion equations keeping a perturbed term representing diffusion; however, they again assume that the F-layer response to a sinusoidal gravity wave is sinusoidal. Numerical methods are employed by these authors to obtain solution of the resulting equations.

Comparison of their results in which diffusion is alternately included and neglected demonstrates that diffusion is an important process in the F-layer. This result is not surprising, however, since the importance of diffusion in F-layer processes has been recognized from the early beginnings of F-layer theory (Ferraro, 1945,1946).

Klostermeyer (1972 a,b) has assumed the same form of the ionospheric response as obtained by Hooke (1968). In these numerical calculations Klostermeyer obtains simultaneous solution of the neutral equations and ionospheric response. Again in this approach the ionospheric response to a sinusoidal gravity wave is assumed to be sinusoidal.

The treatment of F-layer response which we develop in the next two chapters does not suffer from the shortcomings mentioned above. The time dependent behavior of the F-layer is obtained directly by solution; not by assumption as in the perturbation approaches. Unlike Nelson (1968), we retain diffusion and loss processes when obtaining solution so that reasonable comparisons with experiment can be made.

An additional feature of this treatment is that we may also investigate effects of gravity wave on the behavior of 6300Å OI and 5200Å NI emissions. While there have been many theoretical treatments of the response of the F-layer to gravity waves, there have been no published theoretical investigations of the effects of gravity waves on airglow emissions. This has occurred in part because of the various assumptions made by most authors in obtaining solution for the ionospheric response.

The theory of the atomic oxygen emission excited via dissociative recombination has been developed most completely by Peterson, Van Zandt, and Norton (1966). Analytic time dependent solution of 6300Å OI nightglow emission was obtained by Tuan (1969). Hernandez and Turtle (1969) have discussed 5200Å NI emission excited through dissociative recombination.

Chapter 2

Theoretical Formulation

2.1 General Statement of the Problem

A fully consistent treatment of F-layer response which includes effects due to momentum transfer from the neutral constituents in the atmosphere, requires simultaneous solution of the coupled partial differential equations governing the behavior of the neutral and ionized constituents. However, since we are primarily concerned with the response of the F-layer, we will consider only the equations governing the ionized species, and use phenomenology when required. The variables necessary to characterize the behavior of the ionized constituents are their respective number densities, pressures, temperatures, and velocities. These variables are related through the continuity equation, the dynamical equation and the equation of state.

In the absence of disturbance, we consider the atmosphere to be planar, isothermal, and horizontally stratified. We limit our treatment to disturbances for which the F-layer response can be treated using a model requiring only one spatial dimension. This is essentially a statement that horizontal variations of the disturbance have typical scale lengths that are large compared to the vertical half width of the F-layer. For gravity waves we require the horizontal wavelength to be large compared to the half width of the

F-layer.

We will assume ambipolar diffusion for the major ionized constituents. In this assumption the ions and electrons diffuse through the major neutral constituent with the same velocity. Since the ion and electron equations are nearly identical in this approximation, we will work with the ion equations noting that the electron equations are similar.

The ion continuity equation can be written

$$\frac{\partial N_i}{\partial t} + \nabla \cdot (\mathbf{V}_i N_i) = F - L_i \qquad (2\text{-}1)$$

where N_i is the ion concentration, $\mathbf{V}_i$ is the ionic velocity, F is the ion production rate, and L_i is the ion loss rate.

The dynamical equation for the ion motion can be written

$$N_i m_i \frac{D\mathbf{V}_i}{Dt} = e\left[\mathbf{E} + \mathbf{V}_i \times \mathbf{B}\right] \qquad (2\text{-}2)$$

$$+ N_i m_i \mathbf{g} - \nabla P_i - m_i \nu_{in}(\mathbf{V}_i - \mathbf{u})$$

where $\underset{\sim}{E}$, $\underset{\sim}{B}$ are the ambient electric and magnetic fields, $\underset{\sim}{g}$ is the gravitational acceleration, P_i is the ion pressure, ν_{in} is the ion neutral collision frequency, and $\underset{\sim}{u}$ is the neutral velocity. We have neglected momentum transfer between the ion and electron species since they are assumed to diffuse through the major neutral constituent with the same velocity.

The ions are assumed to obey an ideal gas law

$$P_i = N_i KT \tag{2-3}$$

This set of equations (2-1), (2-2), (2-3) and the corresponding electron equations determine the behavior of the ionized constituents, once we have specified information concerning the neutral constituent behavior.

2.2 Ion Drift Velocity Calculation

Considerable simplification of the ion dynamical equation can be made using approximations which are valid at F-layer altitudes. We are primarily interested in developing an analytic treatment of F-layer response which can be used to treat long period, long wavelength disturbance caused by gravity waves or thermospheric winds. For these disturbances we may safely neglect the inertial terms of the dynamical equation. This neglect is legitimate since typical gravity wave periods (of the order of hours) are large compared to the ion gyromagnetic period ($\sim$.06 sec.) and the time interval between collisions suffered by an ion with molecules of the neutral gas ($\sim$3 sec. near the F-layer peak). (Rishbeth and Garriott, 1969). The convective derivative is negligible for motions with spatial scales of the order of a neutral scale height or greater, which we are considering here, unless the ion velocity is of the order of local speed of sound (Hooke, 1968). Under these approximations the ion dynamical equation can be written:

$$
\begin{aligned}
\underset{\sim}{V}_i = \frac{1}{m_i \nu_{in}} \Bigg\{ & e\left[\underset{\sim}{E} + \frac{\nu_{in}\omega_i}{\nu_{in}^2+\omega_i^2}(\underset{\sim}{E}\times\underset{\sim}{1}_b) + \frac{\omega_i^2}{\nu_{in}^2+\omega_i^2}(\underset{\sim}{E}\times\underset{\sim}{1}_b)\times\underset{\sim}{1}_b\right] \qquad (2\text{-}4) \\
& + m_i\nu_{in}\left[\underset{\sim}{u} + \frac{\nu_{in}\omega_i}{\nu_{in}^2+\omega_i^2}(\underset{\sim}{u}\times\underset{\sim}{1}_b) + \frac{\omega_i^2}{\nu_{in}^2+\omega_i^2}(\underset{\sim}{u}\times\underset{\sim}{1}_b)\times\underset{\sim}{1}_b\right] \\
& + m_i\left[\underset{\sim}{g} + \frac{\nu_{in}\omega_i}{\nu_{in}^2+\omega_i^2}(\underset{\sim}{g}\times\underset{\sim}{1}_b) + \frac{\omega_i^2}{\nu_{in}^2+\omega_i^2}(\underset{\sim}{g}\times\underset{\sim}{1}_b)\times\underset{\sim}{1}_b\right] \\
& - \frac{1}{N_i}\left[\nabla(N_iKT) + \frac{\nu_{in}\omega_i}{\nu_{in}^2+\omega_i^2}\left[\nabla(N_iKT)\times\underset{\sim}{1}_b\right]\right. \\
& \left. + \frac{\omega_i^2}{\nu_{in}^2+\omega_i^2}\left\{\left[\nabla(N_iKT)\times\underset{\sim}{1}_b\right]\times\underset{\sim}{1}_b\right\}\right] \Bigg\}
\end{aligned}
$$

where ω_i is the ion gyromagnetic frequency and $\underset{\sim}{1}_b$ is a unit vector along the magnetic field line.

At F-layer altitudes the ion gyromagnetic frequency is known to be nuch larger than the ion neutral collision frequency ($\frac{\nu_{in}}{\omega_i} \sim 10^{-3}$ near the F-layer peak), thus we may drop terms of the order of $\frac{\nu_{in}}{\omega_i}$. The electric field existing at F-layer altitudes is small owing to the F-layer's high conductivity, and will be neglected. With these approximations the ion drift velocity may be written

$$\underset{\sim}{V}_i = \frac{1}{N_i m_i \nu_{in}} \Big\{ N_i m_i \nu_{in} (\underset{\sim}{U} \cdot \underset{\sim}{1}_b) \underset{\sim}{1}_b + N_i m_i (\underset{\sim}{g} \cdot \underset{\sim}{1}_b) \underset{\sim}{1}_b - [\nabla (N_i KT) \cdot \underset{\sim}{1}_b] \underset{\sim}{1}_b \Big\} \tag{2-5}$$

The corresponding electron drift equation can be written, using the previous assumption that $\underset{\sim}{V}_e = \underset{\sim}{V}_i$.

$$\underset{\sim}{V}_i = \frac{1}{N_e m_e \nu_{en}} \Big\{ N_e m_e \nu_{en} (\underset{\sim}{U} \cdot \underset{\sim}{1}_b) \underset{\sim}{1}_b + N_e m_e (\underset{\sim}{g} \cdot \underset{\sim}{1}_b) \underset{\sim}{1}_b - [\nabla (N_e KT) \cdot \underset{\sim}{1}_b] \underset{\sim}{1}_b \Big\} \tag{2-6}$$

In the ionospheric plasma it is always assumed that each unit volume is electrically neutral, at least for dimensions larger than the Debye radius (about 1 cm. in the F-layer). Since the concentration of the minor ionized constituents is small over most of the altitude range of the F-layer, we may write $N_i \sim N_e$. Adding equations (2-5) and (2-6) together and neglecting terms of the order of m_e/m_i, $m_e \nu_{en} / m_i \nu_{in}$, we obtain the following result

$$\underset{\sim}{V}_i = \left\{ D_a \left[\frac{\hat{g} \cdot \underset{\sim}{1}_b}{2H} - \frac{\nabla N_i \cdot \underset{\sim}{1}_b}{N_i} \right] + \underset{\sim}{u} \cdot \underset{\sim}{1}_b \right\} \underset{\sim}{1}_b \tag{2-7}$$

where D_a = ambipolar diffusion coefficient = $2KT/m_i \nu_{in}$

and H = ionic scale height = $KT/m_i g$.

Thus, we obtain the well known result that in the F-layer the ions and electrons are constrained to move along the magnetic field lines.

2.3 Linear Loss Term

Dissociative recombination is the principal loss mechanism over most of the altitude range of the F-layer. The important reaction schemes may be written

$$O^+ + O_2 \rightarrow O_2^+ + O \qquad \gamma_1 \qquad (2\text{-}8)$$

$$O_2^+ + e \rightarrow O + O \qquad \alpha_1 \qquad (2\text{-}9)$$

$$O^+ + N_2 \rightarrow NO^+ + N \qquad \gamma_2 \qquad (2\text{-}10)$$

$$NO^+ + e \rightarrow N + O \qquad \alpha_2 \qquad (2\text{-}11)$$

The rate coefficients are given in Table I. While radiative recombination $O^+ + e \rightarrow O$ occurs, the rate coefficient ($\sim 10^{-12} cm^3 s^{-1}$) is small and it is not important at the altitudes we are considering (Rishbeth and Garriot, 1969).

TABLE I

REACTION RATE COEFFICIENTS

Coefficient	Magnitude at 700° K $cm^3 sec^{-1}$	Reference
γ_1	2×10^{-11}	Donahue (1968)
γ_2	1×10^{-12}	Donahue (1968)
α_1	1×10^{-7} (700/T)	Biondi (1968)
α_2	2×10^{-7} (700/T)	Biondi (1968)

We note that equations (2-9) and (2-11) are exothermic and may produce O and/or N in excited states. These states are de-excited through collision or radiative transition. The latter is responsible for airglow emission.

From the set of reactions (2-8) - (2-11) it is clear that the loss rate of the major ion O^+ may be written

$$L_i = \gamma_1 [O_2] N_i + \gamma_2 [N_2] N_i \tag{2-12}$$

while the loss rate of the electrons is given by

$$L_e = \alpha_1 [O_2^+] N_e + \alpha_2 [NO^+] N_e \tag{2-13}$$

Using equations (2-8) and (2-9) we may write the continuity equation for $[O_2^+]$ as

$$\frac{\partial [O_2^+]}{\partial t} = -\alpha_1 N_e [O_2^+] + \gamma_1 [O_2] N_i \tag{2-14}$$

where we have neglected the divergence term. This approximation has been justified by Peterson et. al. (1966) who have shown that O_2^+ will diffuse only a small distance during its lifetime. We may neglect the time derivative of $[O_2^+]$ provided that the production of O_2^+ does not vary strongly in a characteristic time of $1/\alpha_1 N_e$. This characteristic time is generally smaller than 100 sec. for the altitude range we consider here. Typical time scales for variations in the production of O_2^+ are of the order of hours, hence, we may set $\partial[O_2^+]/\partial t = 0$. Using charge neutrality $N_i \sim N_e$ (Section 2.2), we obtain from equation (2-14)

$$[O_2^+] = \gamma_1 [O_2]/\alpha_1 \tag{2-15}$$

Using an argument similar to that used for the concentration of O_2^+, we may obtain the following result for the concentration of NO^+

$$[NO^+] = \gamma_2 [N_2]/\alpha_2 \tag{2-16}$$

Substitution of (2-15) and (2-16) into (2-13) reveals that the loss rates for the ions and electrons are identical in this approximation.

We may rewrite equation (2-12) as

$$L_i = \gamma_1 \left(1 + \gamma_2[N_2]/\gamma_1[O_2]\right)[O_2] N_i \tag{2-17}$$

Since the ratio $\gamma_2[N_2]/\gamma_1[O_2]$ varies only slowly with altitude (due to the near equality of scale heights for N_2 and O_2) we may define an effective rate coefficient $\bar{\gamma}_1$ which is independent of altitude such that

$$L_i = \beta N_i \tag{2-18}$$

where

$$\beta = \overline{\gamma_1}\,[O_2]$$

In this approximation the loss term is found to be linear and the recombination coefficient β varies with altitude according to the distribution of O_2.

2.4 Continuity Equation

As we have mentioned previously, we consider only those disturbances for which the F-layer response can be treated using a model requiring only one spatial dimension. Substitution of the drift velocity expression into the continuity equation results in the following equation,

$$\frac{\partial Ne}{\partial t} + \frac{\partial}{\partial z}\left[-D_a\left(\frac{\partial Ne}{\partial z} + \frac{Ne}{2H}\right)\cos^2\theta \right.$$
$$\left. + N_e U_y \sin\theta\cos\theta + N_e U_z \cos^2\theta\right] = F - \beta Ne \tag{2-19}$$

Where θ is the angle between the magnetic field and the zenith, $z = h - h_o$ is the difference between the actual height h and some initial position h_o. The y axis of the coordinate system is chosen along the direction of the horizontal component of the magnetic field line. We have assumed for simplicity that the neutral velocity lies in the plane containing the magnetic field line and the zenith.

In general, owing to the perturbations on the atmosphere from the gravity wave, both the diffusion and recombination coefficients are time dependent. To first order approximation we may write

$$D_a(z,t) = D_a(z) + \delta D_a(z,t)$$
$$\beta(z,t) = \beta(z) + \delta\beta(z,t) \tag{2-20}$$

We shall neglect $\delta D_a(z,t)$ in comparison with $D_a(z)$ and $\delta\beta(z,t)$ in comparison $\beta(z)$. although it is relatively easy to include both variations phenomenologically. That this approximation should be good down to about 3 scale heights below the F-layer peak is shown in Appendix A. We will assume the usual forms for β and D_o, $\beta = \beta_o \exp(-pz/H)$ and absorbing the $\cos^2\theta$ factor into the diffusion coefficient $D_a\cos^2\theta = D_o \exp(z/H)$. We will show later that this approximation is consistent with the model for the diffusion coefficient obtained by Shunk and Walker (1970).

2.5 Mathematical Formulation

Introducing a change of variable $x = \alpha \exp(-z/H)$ where $\alpha = 2H(\beta_o/D_o)^{1/2}$ and the transformation $N_e = x^{1/4}\Psi(x,t)$ We may convert equation (2-19) into the following equation

$$\frac{\partial^2\Psi}{\partial x^2} + \frac{3}{16x^2}\Psi - \frac{1}{4}\Psi - \frac{K}{x}\frac{\partial\Psi}{\partial t} = \rho(x,t) \tag{2-21}$$

where

$$\rho(x,t) = \frac{1}{4}\left[\left(\frac{x}{\alpha}\right)^{p-1} - 1\right]\Psi - \frac{KF}{x^{5/4}} - \frac{K}{H}\frac{\partial(\Psi u_z)}{\partial x}\cos^2\theta$$

$$-\frac{K\Phi u_z}{4Hx}\cos^2\theta - \frac{K}{Hx}\left[x\frac{\partial(\Phi u_y)}{\partial x} + \frac{\Phi u_y}{4}\right]\sin\theta\cos\theta$$

and

$$K = H/2(\beta_0 D_0)^{1/2}.$$

In equation (2-21) we have put all of the perturbing influences such as the neutral velocity and the ion production terms into the function $\rho\,(x,t)$. In the absence of such influences and when the gases are perfectly mixed (P=1), we are left with the homogeneous equation giving Chapman-type solutions for a quiet night-time ionosphere.

The homogeneous part of equation (2-21) is identical to the homogeneous equation used in a study of the polar ionosphere under the influence of electron precipitation (Moschandreas and Tuan, 1973). Since this equation is not self adjoint in the time variable, it is necessary that we use the adjoint equation for the Green's function in terms of the dashed variables to obtain formal solution of this equation. Formal solution of equation (2-21) can then be written

$$\Phi(x,t) = K\int_0^\infty\int_{t_0}^{t} G(x,x';t,t')\,\frac{F(x',t')}{x'^{5/4}}\,dx'dt'$$

$$+K\int_0^\infty \frac{G(x,x';t,t_0)\,\Phi(x',t_0)}{x'}\,dx' + \int_{t_0}^{t}\left(G\frac{\partial\Phi}{\partial x'} - \Phi\frac{\partial G}{\partial x'}\right)\Bigg|_{x'=0}^{x'=\infty} dt'$$

$$- \int_0^\infty \int_{t_0}^{t} G(x,x';t,t') \frac{1}{4} \left[\left(\frac{x'}{\alpha}\right)^{p-1} - 1 \right] \Sigma(x',t') \, dx' dt'$$

$$+ \frac{K \sin\theta \cos\theta}{H} \left[\int_0^\infty \int_{t_0}^{t} G \frac{\partial(\Sigma u_y)}{\partial x'} dx' dt' + \int_0^\infty \int_{t_0}^{t} \frac{G \Sigma u_y}{4x'} dx' dt' \right] \qquad (2\text{-}22)$$

$$+ \frac{K \cos^2\theta}{H} \left[\int_0^\infty \int_{t_0}^{t} G \frac{\partial(\Sigma u_z)}{\partial x'} dx' dt' + \int_0^\infty \int_{t_0}^{t} \frac{G \Sigma u_z}{4x'} dx' dt' \right]$$

The Green's function in equation (2-22) may be expressed in closed form as follows:

$$G(x,x';t,t') = \frac{u(t-t')(x x')^{1/4} \left(\frac{2}{\pi}\right)^{1/2}}{2K\left[\sinh\left(\frac{t-t'}{2K}\right)\right]} \cosh\left[\frac{(x x')^{1/2}}{\sinh\left(\frac{t-t'}{2K}\right)}\right]$$

$$\cdot \exp\left[- \frac{\cosh\left(\frac{t-t'}{2K}\right)}{\sinh\left(\frac{t-t'}{2K}\right)} \frac{(x+x')}{2}\right] \qquad (2\text{-}23)$$

where $$u(t-t') = \begin{cases} 1 & (t>t') \\ 0 & (t<t') \end{cases} .$$

The Green's function given by equation (2-23) satisfies homogeneous boundary conditions in the half interval $(0 \le x < \infty)$ corresponding to the full interval for the altitude h, $(0 \le h < \infty)$.

Since the F-layer is basically a Chapman-like function, one of our aims is to use the Laguerre Polynomials whose weighting function is just the Chapman function to analytically approximate the F-layer. A useful advantage of the Green's function as given by equation (2-23) is that it may be expanded into Laguerre Polynomials. The spectral expansion of this Green's function is given by

$$G = \frac{1}{K}\sum_{n=0}^{\infty} \frac{e^{\frac{\omega_n}{K}(t-t')}\,u(t-t')\,(xx')^{1/4}}{\Gamma(n+1)\,\Gamma(n+1/2)}\, e^{-\frac{(x+x')}{2}}\, L_n^{-1/2}(x)\, L_n^{-1/2}(x') \qquad (2\text{-}24)$$

where

$$\omega_n = -(n + 1/4)$$

$$L_n^{-1/2}(x) = \sum_{m=0}^{n} \frac{\Gamma(n+1)\,\Gamma(n+1/2)\,(-x)^m}{\Gamma(n-m+1)\,\Gamma(m+1/2)\,\Gamma(m+1)} \; .$$

The third integral on the right-hand side of equation (2-22) vanishes at $x' = \infty$ and cancels out at $x' = 0$. The fifth integral may be written:

$$\int G \frac{\partial}{\partial x'}(\Sigma u_y)\,dx'dt' = \int \frac{\partial}{\partial x'}\left[G \Sigma u_y\right] dx'dt' + \int \frac{\partial G}{\partial x'} \Sigma u_y\, dx'dt' \qquad (2\text{-}25)$$

The first integral on the right-hand side of equation (2-26) vanishes at the upper limit for x and would vanish at the lower limit provided the amplitude of u_y, u_{yo} is given by

$$u_{yo} \sim \left(\frac{x}{\alpha}\right)^{-q} \quad (0 \leq q < 0.5).$$

The seventh integral may be treated in similar manner. Since we will not consider any value of q greater than 0.49, we may drop these terms.

The first term on the right-hand side of equation (2-22) corresponds to the production of ion pairs. We may rewrite this term as follows:

$$K \int \frac{G F(x',t')}{x'^{5/4}} dx' dt' = \sum_{n=0}^{\infty} \frac{b_n(t,t_0) e^{-\frac{x}{2}}}{\Gamma(n+1)\Gamma(n+1/2)} x^{1/4} L_n^{-1/2}(x) e^{\frac{\omega_n}{K}(t-t_0)} \tag{2-26}$$

where

$$b_n(t,t_0) = \int e^{-\frac{\omega_n}{K}(t'-t_0)} e^{-\frac{x'}{2}} L_n^{-1/2}(x') \frac{F(x',t')}{x'} dx' dt' .$$

The second term on the right-hand side of equation (2-22) is the initial electron density distribution at

$t = t_o$. We may write this as

$$K\int G(x,x';t,t_o)\,\frac{\Xi(x',t_o)}{x'}\,dx' = \sum_{n=0}^{\infty}\frac{a_n(t_o)\,e^{\frac{\omega_n}{K}(t-t_o)}}{[\Gamma(n+1)\,\Gamma(n+1/2)]^{1/2}}\;x^{1/4}e^{-x/2}\,L_n^{-1/2}(x) \qquad (2\text{-}27)$$

where we have assumed that

$$\Xi(x,t) = x^{1/2}\sum_n a_n(t)\,V_n(x)$$

since , form

$$V_n(x) = \frac{e^{-x/2}\,x^{-1/4}\,L_n^{-1/2}(x)}{[\Gamma(n+1)\,\Gamma(n+1/2)]^{1/2}}$$

a complete set.

We may write the following integral equation for the electron density

$$N_e(x,t) = \sum_{n=0}^{\infty}\left\{\left[\frac{a_n(t_o)}{[\Gamma(n+1)\,\Gamma(n+1/2)]^{1/2}} + \frac{b_n(t,t_o)}{\Gamma(n+1)\,\Gamma(n+1/2)}\right]\cdot e^{\frac{\omega_n}{K}(t-t_o)}\,x^{1/2}\,e^{-x/2}\,L_n^{-1/2}(x)\right\}$$
$$-\int_0^{\infty}\int_{t_o}^{t} K(x,x';t,t')\,N_e(x',t')\,dx'dt' \qquad (2\text{-}28)$$

where

$$\mathbb{K}(x,x';t,t') = \sum_{n=0}^{\infty} \mathbb{K}_n(x,x';t,t')$$

and

$$\mathbb{K}_n(x,x';t,t') = \frac{e^{\frac{\omega_n}{\kappa}(t-t')} x^{1/2} e^{\frac{-x+x'}{2}}}{\Gamma(n+1)\,\Gamma(n+1/2)} L_n^{-1/2}(x)$$

$$\cdot \left\{ \frac{1}{4\kappa}\left[\left(\frac{x'}{\alpha}\right)^{p-1} - 1\right] L_n^{-1/2}(x') + \frac{u_y(x',t')\sin\theta\cos\theta}{H}\left[\frac{d L_n^{-1/2}(x')}{dx'} - \frac{L_n^{-1/2}(x')}{2}\right]\right.$$

$$\left. + \frac{u_z(x',t')\cos^2\theta}{H}\left[\frac{d L_n^{-1/2}(x')}{dx'} - \frac{L_n^{-1/2}(x')}{2}\right]\right\} .$$

Chapter 3

Analytical Solutions for Fully Ducted Mode

3.1 Neutral Wave Model

To obtain solution of the integral equation (2-28) it is nesessary to specify some functional form for the neutral velocity. This choice will be dictated both by the experimental observations with which we choose to compare our theoretical results and the desire to obtain analytic solutions.

We shall consider various forms for the neutral wave velocity distribution $\underset{\sim}{U}(z,t)$ for a fully ducted mode as a function of Z ranging from a constant, to various degrees of exponential increase with altitude. For simplicity we will also consider a sinusoidal time dependence for the incident wave. For the long wavelength and long period waves we wish to investigate, we may neglect the vertical component of the neutral velocity relative to the horizontal component (Hines, 1960). Thus, we may write

$$U_z(x,t) = 0. \qquad\qquad (3\text{-}1)$$
$$U_y(x,t) = A\alpha^{q} x^{-q} \cos\omega(t-t_o)$$

where A is the amplitude at $h = h_o$, t_o is some initial time which gives the phase of U_y at $t = t_o$, and q is a variable in the range $(0 \leq q < 1/2)$. When $q = \frac{1}{2}$, equation (3-1) reduces to the classical undamped Hines model (Hines, 1960) which omits ion drag, thermal conduction, and viscosity. In general, q is a function of height. For simplicity in obtaining analytical solution, however, we assume q to be a constant independent of height. Thus, in this model if ion drag, etc. does occur, the value of q would be somewhat less than $\frac{1}{2}$. Fig. 1 shows a plot of the variations of the exponent of the velocity amplitude as a function of altitude when the various frictional effects are taken into account. The models of Volland (1969, a,b) and Testud and Francois (1971) for unducted gravity waves are also shown as a basis of comparison. Obviously our model for q = .3 is in good agreement with Volland's model up to 450 km. The results begin to differ sharply above 500 km. However, the rapid drop in the electron density will make even a large difference unimportant after the necessary integrations in the integral equation are carried out. We shall take up this point again in Chapter 4. The choice of a fully ducted model is also consistent with the experimental observations of TID obtained by Thome (1968) with which we will compare our results. Thome points out that the initial phase velocity measurements of the disturbance $\sim 700\,\mathrm{m/sec}$ suggests the neutral wave is propagating in a fully ducted mode.

3.2 The Single Exponential Solution

For the remainder of this dissertation we shall assume that there are no ion pair production processes and set

Fig. 1. Variation of the exponent of the velocity amplitude as a function of altitude for (1) q = constant (0.3) (full line), (2) Volland's gravity wave model (-------), (3) Testud and Francois' gravity wave model (-.-.-).

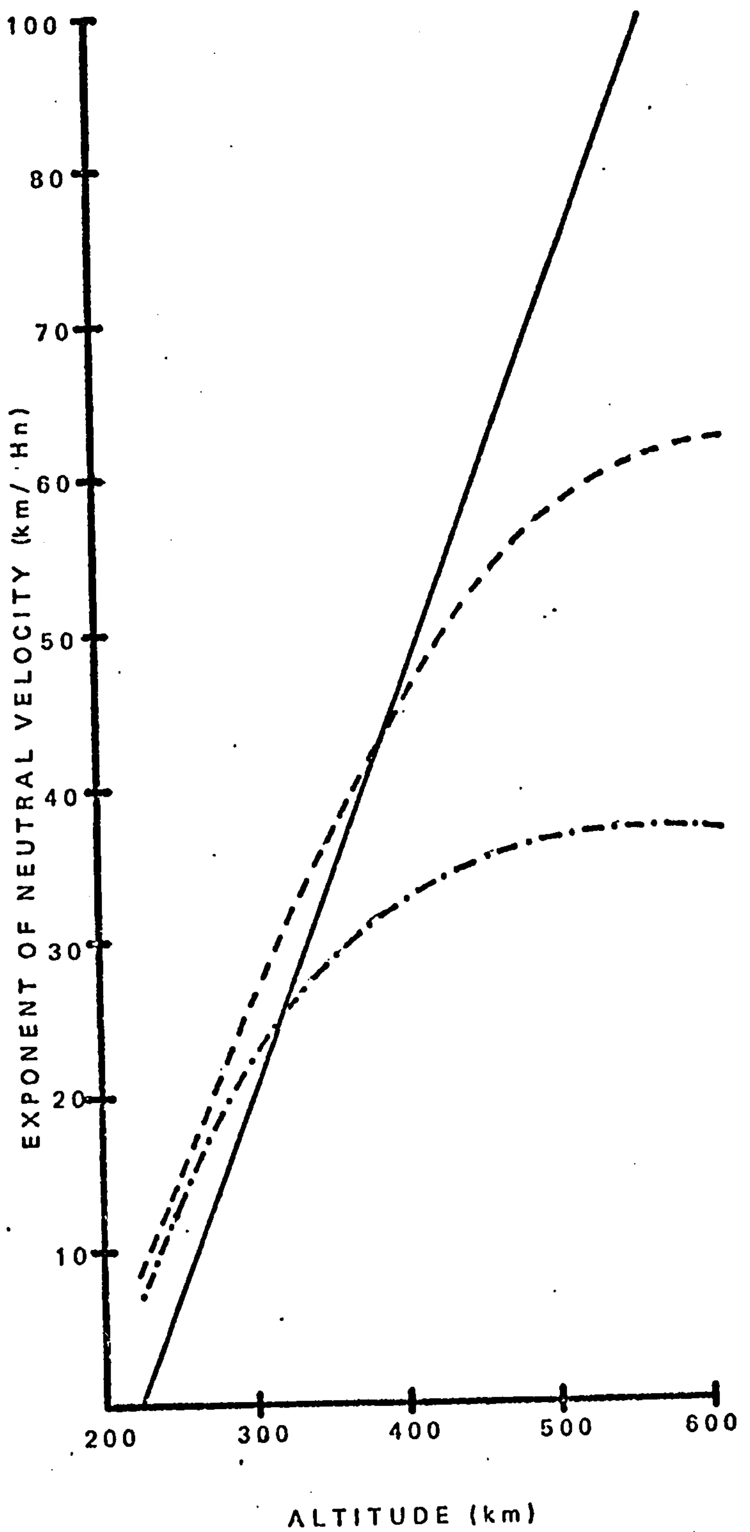

100
80
70
60
50
40
30
20
10
EXPONENT OF NEUTRAL VELOCITY (km/ Hn)
200
300
400
500
600
ALTITUDE (km)

$b_n(t, t_o) = 0$. The formalism can be trivially altered to include this effect but since the experimental observations were taken during late afternoon and evening conditions we shall neglect the production for simplicity. The integral equation (2-28) has a solution in closed form if we take the long time limit $(t >> t_o)$ for the inhomogeneous term and approximate the kernel by the $n = 0$ term. Since, as will be seen, a fair amount of physics is already contained in this special solution, we shall consider this problem in some detail.

With the above mentioned approximations, the integral equation (2-28) becomes

$$N_e(x,t) = \frac{a_o}{\pi^{1/4}} e^{\frac{\omega_o}{K}(t-t_o)} x^{1/2} e^{-x/2} - \frac{e^{-x/2} x^{1/2}}{\pi^{1/2}} \int e^{\frac{\omega_o}{K}(t-t')} e^{-x'/2} \tag{3-2}$$

$$\cdot \left\{ \frac{1}{4K}\left[\left(\frac{x'}{\alpha}\right)^{p-1} - 1\right] - \frac{A \sin\theta \cos\theta}{2H}\left[\left(\frac{x'}{\alpha}\right)^{-q} \cos\omega(t'-\bar{t}_o)\right]\right\} N_e(x',t')\,dx'\,dt'$$

Integrating over the x', t' coordinates for each term in the iteration of (3-2) we obtain an infinite series which can be summed into closed form,

$$N_e = \frac{a_o \alpha^{1/2}}{\pi^{1/4}} e^{-\left(\frac{Z}{2H} + \frac{\alpha}{2} e^{-\frac{Z}{H}}\right)} e^{\left[-\lambda_o(t-t_o) + B(q)\sin\omega(t-t_o)\right]} C(q, t_o, \bar{t}_o) \tag{3-3}$$

where

$$\lambda_0 = \frac{1}{4K}\left\{1 + \frac{1}{\pi^{1/2}}\left[\alpha^{1-p}\,\Gamma(p+1/2) - \Gamma(1+1/2)\right]\right\}$$

$$B(q) = \frac{A\,\alpha^{q}\sin\theta\cos\theta\,\Gamma(3/2-q)}{2\pi^{1/2}\,\omega\,H}$$

$$C(q,t_0,\bar{t}_0) = e^{-\left[B(q)\sin\omega(t_0-\bar{t}_0)\right]}$$

Thus, in this approximation, we have a simple Chapman function multiplied by an oscillatory exponential time decay.

In the limit when there is no TID, the expression given by equation (3-3) will reduce to the corresponding expression for a quiet ionosphere (Tuan, 1968; Moschandreas and Tuan, 1973). The disturbance due to the sinusoidally varying neutral atmospheric gravity wave is given by the last term in the exponent on the right-hand side of equation (3-3). One interesting feature of this expression is that even though the incident wave continues without attenuation, the response of the F-layer dies away exponentially as the F-layer decays. This decay occurs in such a way that the percentage oscillation obtained in comparison with the decay in the absence of the wave is constant. Since the time dependence comes from a single exponential, we shall henceforth refer to it as the "single exponential solution" and denote it by N_o. A plot of this solution against an experimental result of Thome (1968) is made in Fig. 2 for an altitude of 350 km. We have assumed that the gravity wave has a period of about 3 hours, as well as reasonable values for the various other parameters. From Fig. 2 we see that the experimental oscillations decrease in proportion to the average electron density, suggesting just the type of exponential time behavior given by the theory. In fact, on a log plot of the experimental electron density, Thome (1968) has shown that the oscillations continue without any attenuation until well past 2400 hours local time which seems to suggest a continuous wave generation throughout this period without any significant damping with time.

The result also shows that the neutral wave which is assumed to be completely ducted would have no effect on the ionosphere at the magnetic pole and equator when the $\sin\theta$ $\cos\theta$ factor in the oscillating term vanishes.

The behavior of the decay of the F-layer for different scale-height factor ρ $(1 \leq \rho \leq 2)$ has already been discussed in some detail (Tuan, 1968). In general, the decay time increases as p approaches 2 when we have the gases closer to diffusive equilibrium. In equation (3-3) this would decrease the first term in the exponent at any given time relative to the sinusoidal oscillation. Thus, the effect of the oscillation is enhanced when the gases are in diffusive equilibrium, while the overall decay rate is slower.

Fig. 2. A comparison of observed normalized electron density (------) and the "single exponential" theoretical solution, (full line) against time.

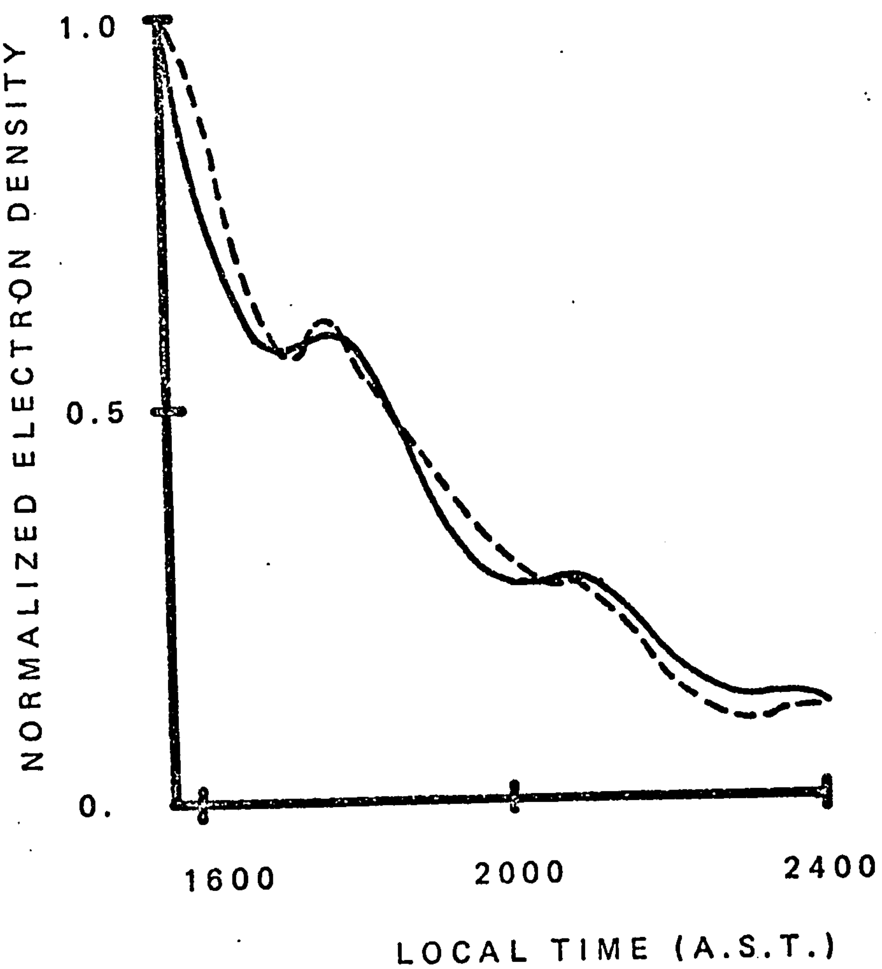
1.0
0.5
0.
NORMALIZED ELECTRON DENSITY
1600
2000
2400
LOCAL TIME (A.S.T.)

We have chosen to vary the vertical distribution of the neutral wave velocity amplitude in such a way that it is fixed at h_o. If h_o is below h_m, the peak position, α is greater than unity. An increase in q would increase the oscillation of the electron density. However, should we choose to fix the velocity amplitude at say h_o, such that $h_o > h_m$ then an increase in q would decrease the oscillation since the major portion of the electrons would be below h_o where the velocity amplitude has been decreased following an increase in q.

Equation (3-3) gives an immediate and simple picture of the decay of the F-layer under the influence of a TID. We note that even in this approximation the response of the F-layer to a sinusoidal gravity wave is neither sinusoidal nor periodic. However, equation (3-3) is too naive to explain some of the more intricate features of the disturbance. For instance, it does not show the vertical oscillation of the h_mF2. The failure to show this is due to the approximation made in the kernel of the integral equation. Even in the long time limit ($t \gg t_o$) we cannot neglect the $n \neq 0$ terms, since the time variable t' is integrated all the way to t' = t when the time exponential $\exp \frac{\omega_n}{K}(t-t')$ goes to unity for all n.

3.3 The More General Solution

To obtain a more general analytic approximation which will include the $n \neq 0$ terms in the kernel of our integral equation (2-28) we use the simple exponential solution which is the exact solution for the kernel $\mathbb{K}_0(x,x';t,t')$ as the zeroth order approximation and iterate our integral equation. Thus, we rewrite equation (2-28) in terms of the single exponential solution N_0

$$N_e = (N_0 - \mathbb{K}_0 N_0) + (\mathbb{K}_0 + R) N_0 \tag{3-4}$$

where

$$R = \sum_{n=1}^{\infty} \mathbb{K}_n(x,x';t,t')$$

Iterating equation (3-4) and neglecting all quadratic and higher order terms in the kernel, we obtain

$$N_e \sim N_0 + R N_0 \tag{3-5}$$

The analytic approximation given by the right-hand side of equation (3-5) is based on the assumption that N_0 is already a good zeroth order approximation to N_e and that R is not a big correction to K_0. Putting in the expressions for N_0 and R and integrating over the coordinates we obtain

$$N_e \sim \frac{a_o}{\pi^{1/4}} x^{1/2} e^{-x/2} c(q,t_o,\bar{t}_o) \exp\left[-\lambda_o(t-t_o) + B(q)\sin\omega(t-\bar{t}_o)\right]$$

$$- \frac{a_o}{\pi^{1/2}} \sum_{n=1}^{\infty} \frac{e^{-x/2} x^{1/2} L_n^{-1/2}(x)}{\Gamma(n+1)\,\Gamma(n+1/2)} \left[\frac{1}{4K} P_n(q,p,\omega,t)\, S(n,p)\right.$$

$$\left. + \frac{A\alpha^q \sin\theta \cos\theta}{H} R_n(q,p,\omega,t)\, Q(n,q)\right] \quad (3\text{-}6)$$

where

$$P_n = \int_{t_o}^{t} e^{\frac{\omega_n(t-t')}{K}} e^{-\frac{\left[\lambda_o(t'-t_o) - B(q)\sin\omega(t'-t_o)\right]}{c(q,t_o,\bar{t}_o)}} dt'$$

$$R_n = \int_{t_o}^{t} e^{\frac{\omega_n(t-t')}{K}} e^{-\frac{\left[\lambda_o(t'-t_o) - B(q)\sin\omega(t'-t_o)\right]}{\cos\omega(t'-\bar{t}_o)\, c(q,t_o,\bar{t}_o)}} dt'$$

$$S(n,p) = \frac{\alpha^{1-p}\,\Gamma(n-p)\,\Gamma(p+1/2)}{\Gamma(-p)} - \frac{\Gamma(n-1)\,\Gamma(1+1/2)}{\Gamma(-1)}$$

$$Q(n,q) = \frac{\Gamma(q+n-1)\,\Gamma(3/2-q)}{\Gamma(q)}\left[\tfrac{1}{2}(1-q) - n\right]$$

The functions $S(n,p)$ and $Q(n,q)$ have been put in closed form and have the property

$$S(n,\ p=1) = 0. \qquad \text{For all } n$$

$$S(n,\ p=2) = 0. \qquad \text{For all } n \geq 3$$

$$Q(n,\ q=0) = 0. \qquad \text{For all } n \geq 2$$

The corrections to the single exponential solution are given by the infinite sum on the right-hand side of equation (3-6) which reduces to only a few terms for a gas either perfectly mixed or in diffusive equilibrium and for a constant velocity amplitude independent of height ($q = 0$).

It is clear from the analytic expression given by the right-hand side of equation (3-6) that the oscillation of the electron density varies with height in such a way that the phase of the oscillation also varies.

The first term on the right-hand side of equation (3-6) is the single exponential approximation and shows oscillation in the magnitude of the electron density without any peak motion. The second term is a sum of Laguerre Polynomials and provides the vertical oscillation of the profile. The functions P_n and R_n both oscillate with frequency ω with the difference that R_n may change sign as time varies but P_n remains positive for all times. As $\omega \rightarrow 0$, both P_n and R_n become monotonic functions of time and all oscillations vanish from the expression given by equation (3-6).

We should point out that the only parameters associated with the F-layer are the scale height and the scale-height factor. The latter is restricted to values between P=1 and P=2, while values for the former have been given which can vary by as much as a factor of 6. Since almost any electron density profile can be fit with some scale height which essentially controls the thickness of the F-layer, we need to have either an independent means of measuring the scale height or sufficient experimental data available to restrict its freedom of choice. For this reason we have chosen to compare our theory with the experimental results of Thome (1968) where a large amount of detailed experimental data has been simultaneously measured. As will be shown later the range of the scale height will be sharply restricted and can not exceed 60 km.

The variation of the neutral wave velocity amplitude as a function of height is controlled by the parameter q. Fig. 3 shows the comparison of N_e for q = 0, 0.27 and 0.49 at four different altitudes. Here we have used a scale height of 60 km., a scale height factor of 1.22 and a gravity wave amplitude at h_o = 309 km. of 106 km/hr. It is easy to see that the constant amplitude gravity wave (q = 0) may produce at lower altitudes, say 210 km., greater oscillation; but at higher altitudes, the constant amplitude wave produces significantly less than either of the amplitudes which increase exponentially with height. The wave with the largest exponential increase (q = 0.49) produces the greatest oscillation at say, 510 km.

Fig. 3. Normalized electron density is plotted against time for (1) $q = 0$ (.-.-), (2) $q = 0.27$ (------), (3) $q = 0.49$ (full line).

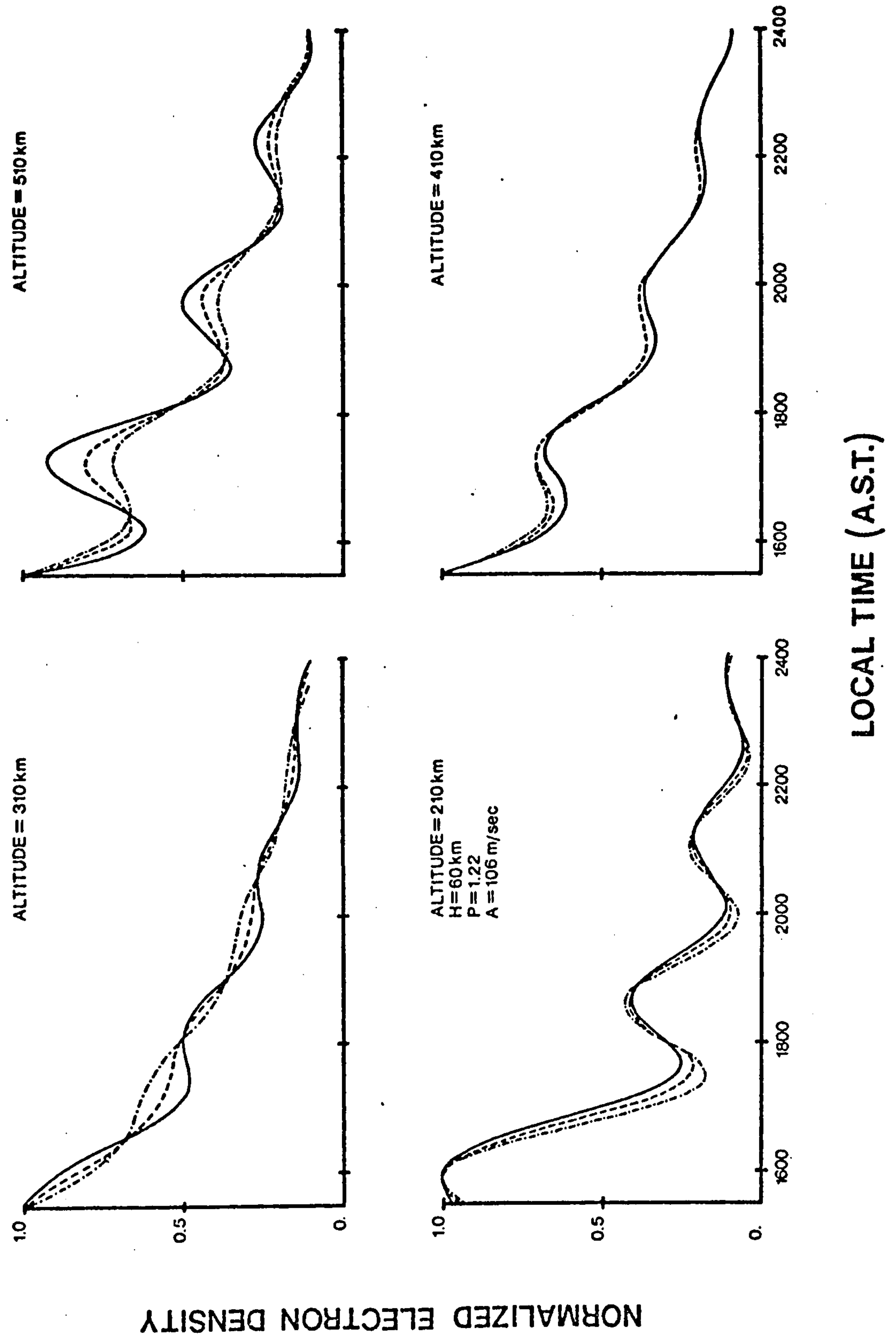
ALTITUDE = 310 km
ALTITUDE = 510 km
ALTITUDE = 210 km
H = 60 km
P = 1.22
A = 106 m/sec
ALTITUDE = 410 km
NORMALIZED ELECTRON DENSITY
1.0
0.5
0.
1600
1800
2000
2200
2400
LOCAL TIME (A.S.T.)

A more interesting phenomenon is the occurrence of a phase change in the electron density oscillation at about 310 km., where the oscillations are considerably less in amplitude than elsewhere. Below this altitude at 1730 hours a trough occurs for all three q values while above this altitude a crest occurs. Since at q = 0.27 the curve shows the least structure, we may conclude that the phase change position varies with the q value and that 310 km. is closest to the position of phase change for q = 0.27. The q = 0 curve obviously has already gone through the position of phase change while the q = 0.49 curve has not yet reached its position of phase change and must occur somewhat higher. In general, as we will show later, the position of phase change is time dependent for each value of q.

The physical reason for the phase change can be readily seen as follows. At any altitude owing to collision with neutral particles there will be some ions flowing out of a given volume while others would flow in. The net increase or decrease of ions would depend on the shape of the electron density distribution at that particular altitude as well as the ionic velocity. Thus, for a constant amplitude neutral wave, the position of phase change would occur at the altitude of the peak electron density. For an amplitude which increases with height the position for phase change would generally be slightly above the peak position. This is born out by the analysis on q variation where the q = 0 curve appears to have the lowest phase change position and the $q = 0.49$ curve seems to have the highest. Since the altitude of the peak electron density is time dependent, the position of the phase change is also time dependent.

Chapter 4

Detailed Comparison Between Theoretical Results and Experiment

4.1 Electron Density Variation at Different Altitudes

A comparison of the theoretical electron density given by equation (3-6) is made with the experimental results of Thome (1968) for six different altitudes (Fig.4) from 206 km. to 567 km. We have taken h_o = 223 km., $\beta(h_o)=3.1\times10^{-4}\,\text{sec.}^{-1}$, $P=1.14$ $D_a(h_o)=3.1\times10^{9}\,\text{cm}^2\text{sec.}^{-1}$, $\alpha=4.11$ and a scale height of 50 km. For the neutral gravity wave we choose $A(h_o)$ = 14.4 m sec^{-1} and q = 0.3. The choice of these parameters is not arbitrary and will be discussed in more detail in Section 4.4. The comparison can only be approximate since we are assuming that the incident neutral wave is sinusoidal with constant frequency. Considerable physical insight can be gained through the theoretical analysis, however, even if the theory does not fit the experiment exactly. This insight is gained through the manifestation of certain general features common to both theory and experiment. The first common feature is that the oscillation amplitude seems to decrease with time in proportion to the magnitude of the average electron density at all altitudes. In this respect the more general result given by equation (3-6) is no improvement over the single exponential solution. Perhaps we should add that neither solution can be obtained using perturbation methods where the undisturbed electron density is assumed to be time

Fig. 4. Comparison of the variarion of observed (------) and theoretical (full line) electron density as a function of local time (A.S.T.) for six different altitudes.

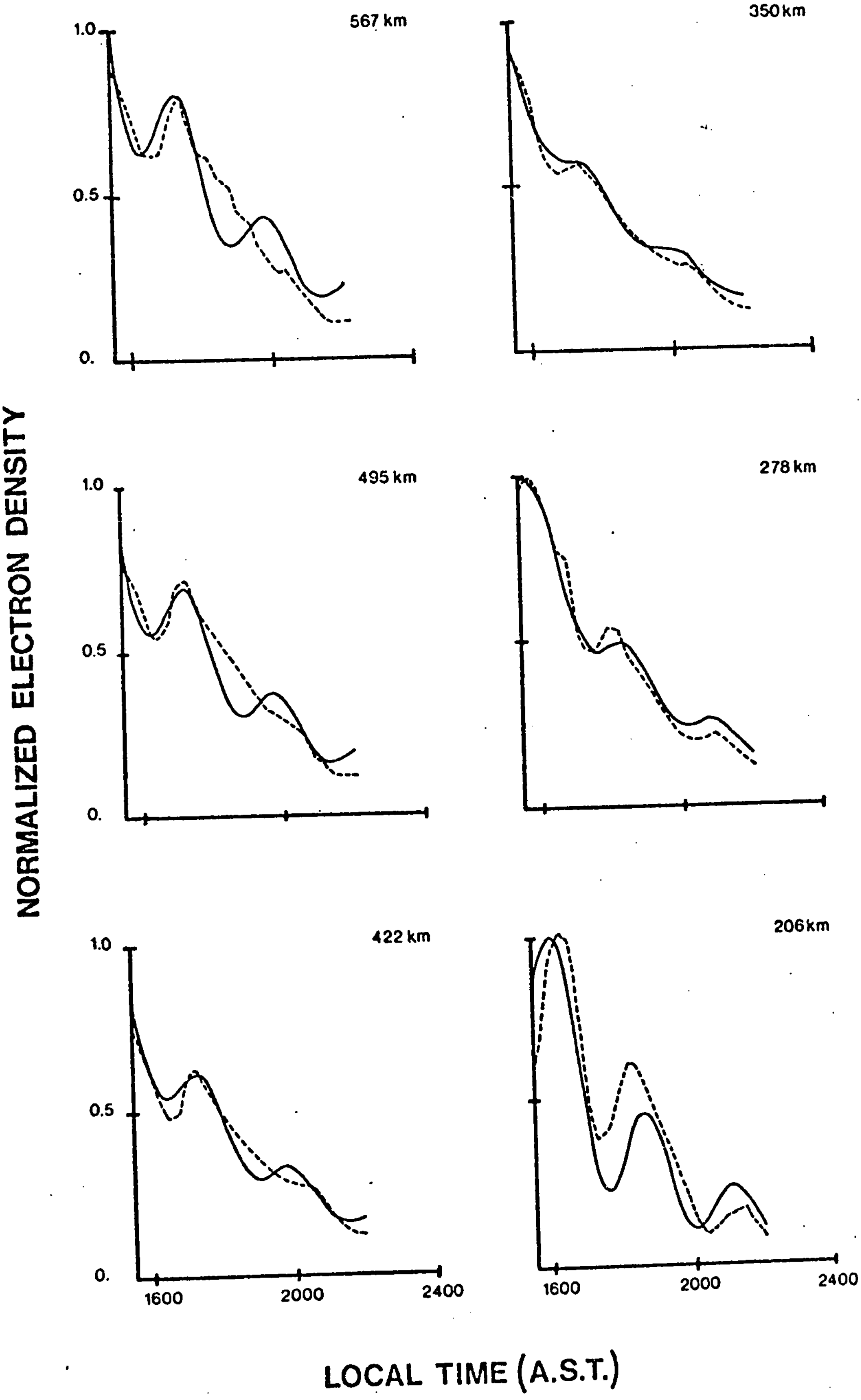
567 km
350 km
495 km
278 km
422 km
206 km
1.0
0.5
0.
1600
2000
2400
NORMALIZED ELECTRON DENSITY
LOCAL TIME (A.S.T.)

independent (Thome, 1968; Testud and Francois, 1971; Hooke, 1968).

The second interesting feature common to both is that the amplitude of the oscillation is very large at low altitudes and gradually decreases to a minimum at 350 km. and increases again above this height. The physical reason for this behavior is that below 300 km. the electron density begins to drop off sharply as an exponential of an exponential. Consequently, a relatively small motion along the magnetic field line would result in large fluctuations of the electron density. The effect is similar to Hooke's large fluctuations for the solar flux (Hooke, 1968). At about 300 km. the electron density reaches a maximum and the variation of the electron density with altitude in this region is relatively small. Hence, the fluctuation is also small. Above 300 km. we have another drop. This time however the drop is much less steep, being just a simple exponential. This drop produces another increase in fluctuation. If we were to use Hine's (1960) original undamped gravity wave model and set q = 0.5, we would obtain much greater oscillation (Fig. 3) above 500 km. However, the best fit for the experimental result of Thome requires a q value of about 0.3. We should perhaps mention that with this q value the amplitude of our gravity wave would increase with altitude as exp $k_2 z$ where $1/k_2 = 167$ km. This is very close to Thome's undamped two layer model where $1/k_2 = 170$ km. Thome has taken measurements which extend above 700 km., however, at these altitudes the signal to noise ratio is such that it becomes relatively difficult to distinguish the oscillations from the noise. Even at these high altitudes damping effects appear to be relatively unimportant.

In Fig. 5, the root mean square deviation from the mean electron density is plotted as a function of altitude. The theoretical curve shows a minimum at about 325 km. which is a little higher than the time averaged peak position (about 300 km.). This difference occurs because the position of minimum deviation should approximately coincide with the position of phase change. The phase change position, as already mentioned in Section 3.3, would occur above the peak electron density due to the exponentially increasing velocity amplitude.

The maximum of the luminosity profile generally occurs below the altitude of the peak electron density (Tuan, 1969). Because the electron density drops sharply in this region the percentage fluctuations of the electron density are large and we would expect to see large fluctuations occur in the magnitude of the peak lumimosity value. Fluctuations observed in the airglow intensity would not be expected to be this large, however, because of the integration over the entire column of atmosphere. We will discuss this further in Chapter 5.

Above 500 km. both experimental and theoretical curves

Fig. 5. Log of r.m.s. deviation from mean electron density for both observed (circles joined by dashed line) and the theoretical (full line) results against altitude.

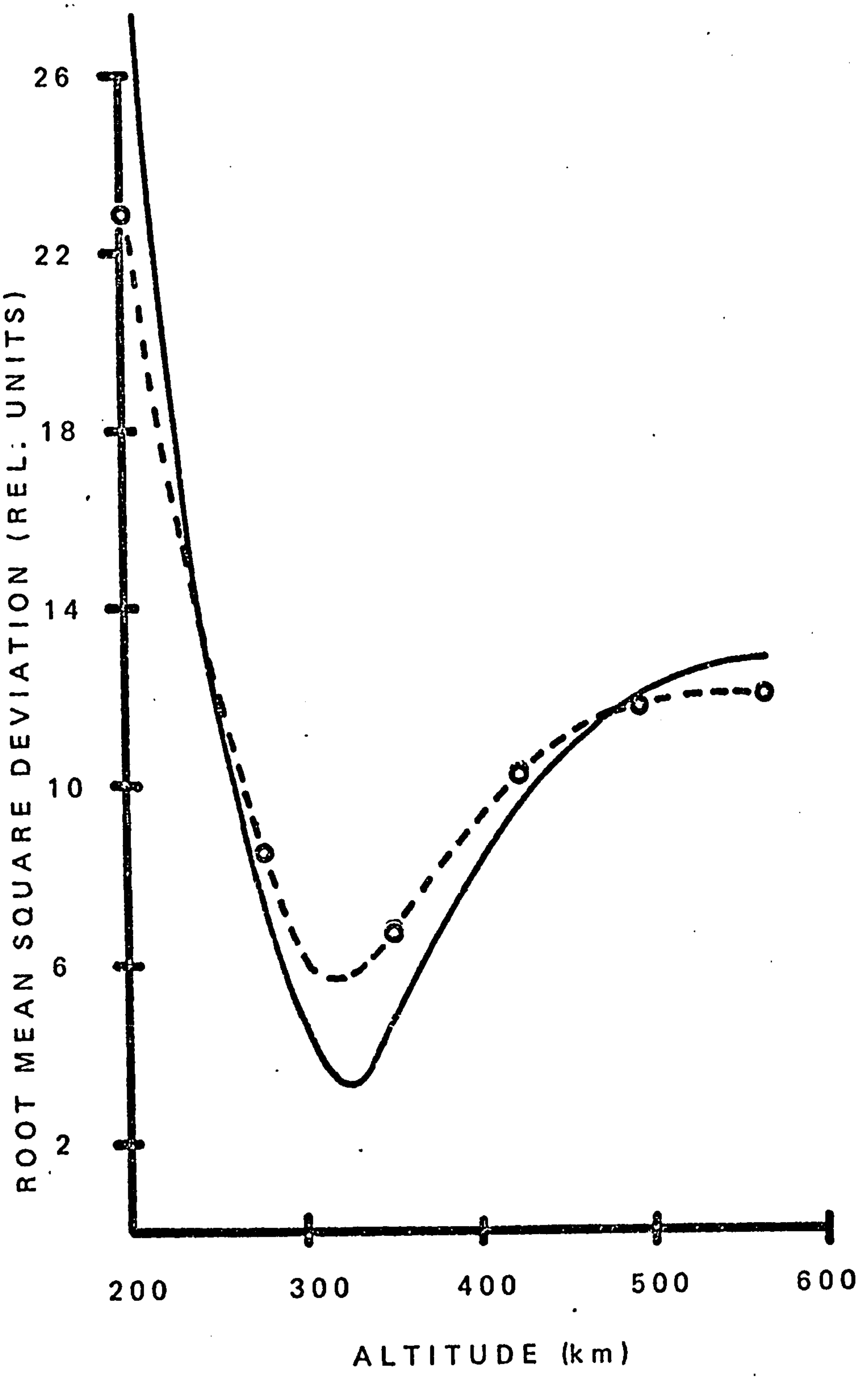
ROOT MEAN SQUARE DEVIATION (REL. UNITS)
26
22
18
14
10
6
2
200
300
400
500
600
ALTITUDE (km)

tend to a constant value in root mean square fluctuation. Damping of the neutral wave should eventually bring this down. However, since we are dealing with wavelengths of the order of 1500 km., we should not expect to see a significant effect within the range of altitude under consideration. This feature is demonstrated by Thome's (1968) experimental observations which seem to indicate unattenuated fluctuation up to at least 700 km.

4.2 Change of Phase in Electron Density Oscillation

In this section the word change of phase has to be used in a rather approximate sense since we are not dealing with sinusoidal waves, in fact we are not even dealing with periodic waves. However, if we look at the experimental results of Thome given in Fig. 4, it is clear that a trough in the oscillation at about 1730 hours L.T. at 206 km. disappears at an altitude of about 350 km. and becomes a crest which increases in magnitude as we move up in altitude. A similar phenomenon occurs at 2030 hours. At 1830 a much less pronounced phenomenon occurs for a crest which disappears at about 350 km. We can thus assume that somewhere between 350 km. and 278 km. a "node" occurs in the oscillation. The terminology is not precise and the change in the phase of the oscillation actually takes place continuously as we move up in altitude. However, if we simply plot the deviation from mean electron density at say 1730 hours L.T., we obtain from Fig. 6 a point of zero oscillation at about 325 km. At this point the theoretical and the experimental curves coincide. The "node" occurs when the number of electrons swept out of a given volume by the neutral wave is equal to the number of electrons swept in and is itself a function of time since the electron density profile is oscillating. Due to the general night-time decay of the F-layer, it is not a periodic function of time.

To further analyse the phase change as a function of height we have plotted in Fig. 7 the time variation of the crest against altitude beginning at 567 km. when the theoretical crest is at 1715 hours. The zero of the time scale indicates when the oscillation is in phase with the neutral wave. For the theoretical curve the electron density oscillates in phase with the neutral wave at about 305 km. Since we have no means of determining the actual phase of the neutral gravity wave, we have also plotted the experimental results on the same curve showing a comparison of theory and experiment when normalized to the same time scale. For instance, at 250 km. the crest of the electron density is about 0.45 hours ahead of the crest of the neutral wave while at 400 km., the crest is 0.73 hours behind the neutral wave. A crest in the neutral wave is defined as maximum neutral particle velocity in a direction which would drag the ions up the magnetic field lines.

The physical reason for the difference in phase is easy

Fig. 6. The log of amplitude deviation from mean electron density at 1740 hours (A.S.T.) for observed (circles joined by dashed line) and theoretical (full line) results.

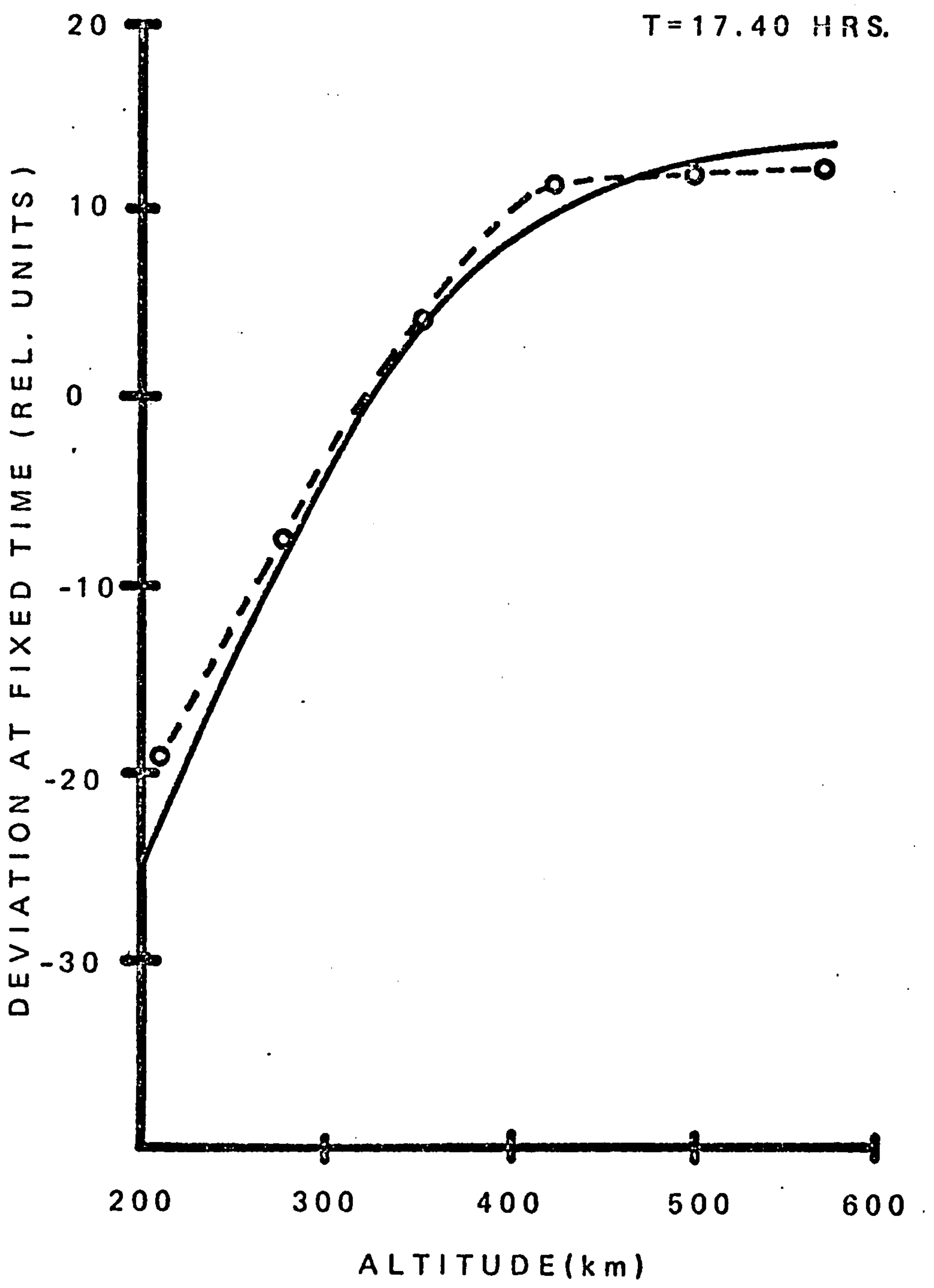
T=17.40 HRS.
20
10
0
-10
-20
-30
DEVIATION AT FIXED TIME (REL. UNITS)
200
300
400
500
600
ALTITUDE(km)

Fig. 7. The phase of the crest of the electron density (expressed in hours ahead of, or behind the crest of the neutral wave) is plotted against height for observed (circles joined by a dashed line) and theoretical (full line) results. At zero hours the electron density oscillates in phase with the neutral wave and this occurs at about 320 km.

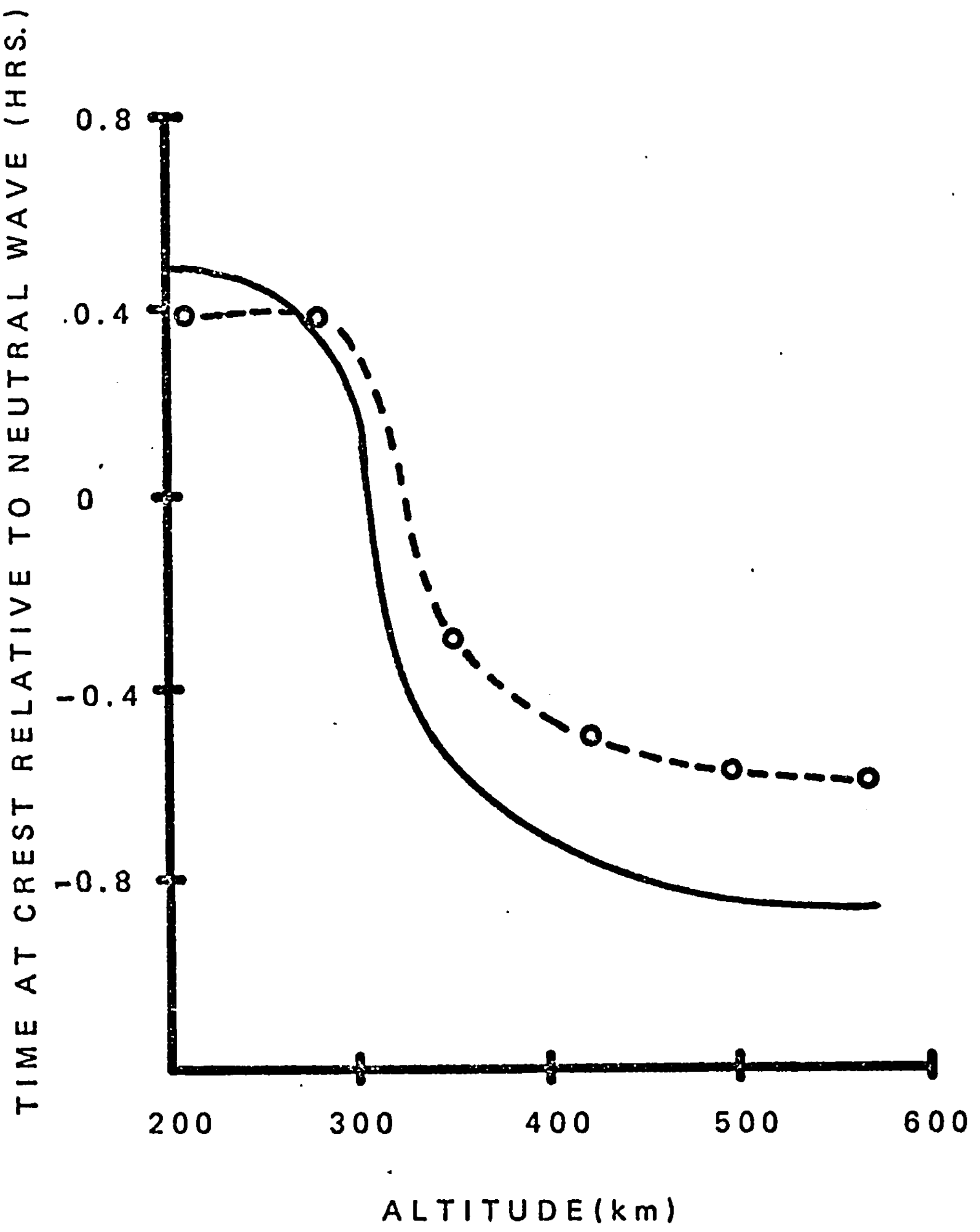
TIME AT CREST RELATIVE TO NEUTRAL WAVE (HRS.)
0.8
0.4
0
-0.4
-0.8
200
300
400
500
600
ALTITUDE(km)

to see. If the electron density was independent of altitude and the neutral wave amplitude was also independent of altitude ($q = 0$), then the electrons would move up and down the field lines in phase with the neutral wave. The change in phase is due to variations in diffusion and recombination rates with height as well as the shape of the electron density profile. Below the F2 peak an upward motion of the ions may cause a net depletion of ions at some altitude, while above the F2 peak an upward motion would cause a net increase of ions.

From Fig. 6, one sees that above 500 km., both the observed and the theoretical deviation from mean electron density tend toward constant values. Theoretically, this can be seen from the right-hand side of equation (3-6) in which, if we factor out the Chapman function $\chi^{1/2} e^{-\chi/2}$, the infinite sum would tend to a fixed value for any given time as $\chi \rightarrow 0 \, (z \rightarrow \infty)$. This is in agreement with the experimental results of Thome (1964). Our results show that the limiting value at great height is time dependent in agreement with Thome (1964).

Thome (1968) has pointed out that a change of phase in the oscillation of the electron density exists and can be understood physically but has not made a detailed theoretical study. Hooke (1968), Testud and Francois (1971), and Klostermeyer (1972 a,b) have used similar perturbation approaches to obtain phase variation in their theoretical treatments. Unlike these methods, our approach is fully time-dependent and the phase change at a particular time as shown in Fig. 6 has a node whose height is itself time dependent. In fact the whole curve, both theoretical and experimental, will vary with time. We are also able to investigate the actual relative phase between the electron density oscillation and the neutral gravity wave as a function of altitude (Fig. 7). Once again we like to mention that the word "phase" is used in two senses in Fig. 6 and Fig. 7. The "phase" used with reference to Fig. 6 describes the instantaneous deviation from mean decay of the electron density as a function of height. Klostermeyer has used the word "phase delay" to describe this. Our Fig. 7 actually describes the phase variation in its usual sense.

4.3 Peak Electron Density Oscillation

The experimental and theoretical variations in peak position of the electron density as a function of time are plotted in Fig. 8. The experimental curve shows a sharp rise after 2300 local time which the theory does not show. This is due to our approximation of the initial electron density distribution by a single Chapman function rather than a linear combination (i.e. $a_n = 0, n \geq 1$). The rise in peak electron density at night is a well understood phenomenon and has already been discussed in some detail for the quiet ionosphere (e.g. Tuan, 1968). For simplicity, we have

Fig. 8. Variation of the height of peak electron density with time for observed (dashed line) and theoretical (full line) values.

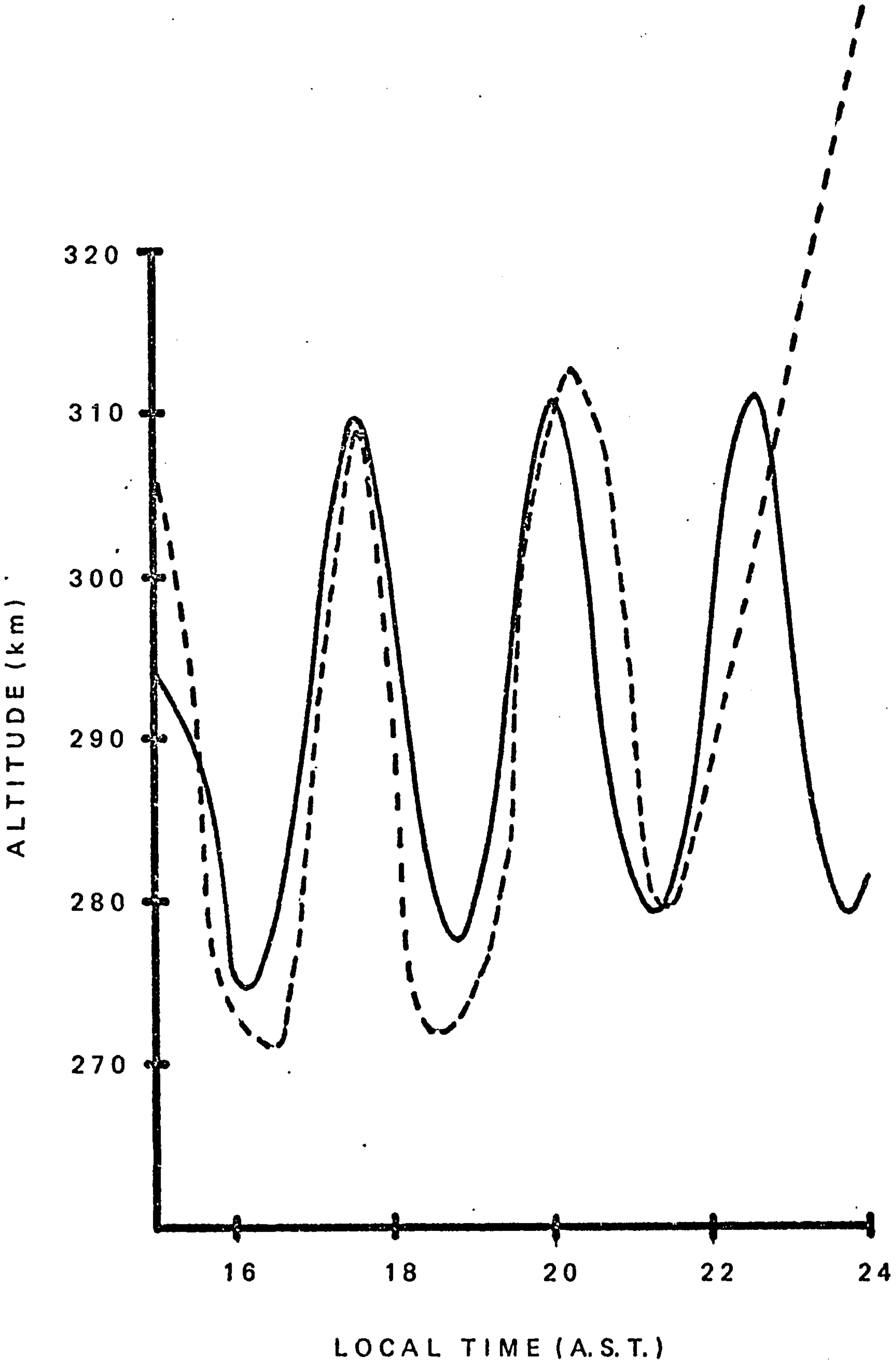
320
310
300
290
280
270
ALTITUDE (km)
16
18
20
22
24
LOCAL TIME (A.S.T.)

considered only one Chapman term in the inhomogeneous part of the integral equation.

There is also a steady rise in the oscillation of the peak electron density between 1500 and 2200 hours local time. The slope of this rise is determined by the scale-height factor p. In general the greater the value of p, the steeper the slope. This can be seen very clearly from equation (3-6). The rise in the average peak position is independent of the gravity wave. Let us set A = ω = 0. and factor out the exponential time decay factor $\exp[-\lambda_0(t-t_0)]$ from the entire right-hand side of equation (3-6). Now instead of $P_n(q_0, p, \omega, t)$ we have $\exp[-\lambda_0(t-t_0)]\ P_n(q, p, \omega, t)$ which is zero at $t = t_0$ and approaches a constant at large t (the term containing R_n now vanishes). This means that at $t = t_0$ the peak position is given by the simple Chapman term but at $t > t_0$, the peak rises until it eventually reaches a steady value as $t \to \infty$.

The steady state peak position is determined by the values of β_0, D_0 , and p. However, for p = 1 the term containing P_n vanishes and the steady state peak position remains the same as that at $t = t_0$. It is easy to see that the rate of increase of peak altitude depends on p.

If we look at the results of Thome in Fig. 8, we find a gentle rise in peak height from 1600 to 2200 followed by a sharp rise about 2300. By matching the slope of the gentle rise in the peak height of the experimental results we have an independent means of determining p. The value obtained in this manner is p = 1.14.

4.4 Inter-Relations between Ionospheric Parameters

In choosing the parameters for the theoretical results just mentioned, we tried to keep to measured or computed values whenever such values are obtainable. Since so many measurements are made simultaneously, all of the parameters are rigidly tied down. Throughout much of the analysis we did not have the experimental electron density profile. Consequently, the scale height H which is a direct measure of the thickness of the F-layer is not known. The rate of increase of fluctuation on either side of peak electron density is so large, however, that H cannot exceed 50 km. We can always increase the fluctuation at all altitudes by increasing the amplitude of the traveling wave but there is no other consistent way to adjust the rate of increase on both sides of the peak except by changing the scale height.

The parameters for the F-layer are not arbitrary and must at least approximately satisfy the following simultaneous equations:

$$K = H/2\left[\beta(h_0)\,D_a(h_0)\right]^{1/2}$$

$$\alpha = 2H\left[\beta(h_0)/D_a(h_0)\right]^{1/2}$$

$$h_m - h_0 = H \operatorname{Log}_e \alpha$$

$$\lambda_0 = \frac{1}{4K}\left[1 + \frac{\alpha^{1-p}\,\Gamma(p+1) - \Gamma(1+\frac{1}{2})}{\pi^{1/2}}\right] \qquad (4\text{-}1)$$

h_m is the time averaged peak position for electron density and is fixed by experiment to a value of about 295 km. is fixed to about 0.25 per hour from the experimental decay time. With the requirement that the diffusion coefficient be compatible with the results of Schunk and Walker (1970) and a choice of 223 km. for h_0 dictated by convenience as already mentioned in Section 3.2, (i.e. $h_0 < h_m$), we obtain the value of $3.1 \times 10^{-4}\ \mathrm{sec}^{-1}$ for $\beta(h_0)$ and a value of $3 \times 10^{9}\ \mathrm{cm}^2\ \mathrm{sec}^{-1}$ for $D_a(h_0)$.

These values are obtained from equation (4-1). The value for the ambipolar diffusion coefficient is in fact only 20% below the Schunk and Walker (1970) value at the same altitude. The recombination coefficient at $h_0 = 400\ \mathrm{km}$ gives a value of $0.56 \times 10^{-5}\ \mathrm{sec}^{-1}$ which compares well with a value of $1.5 \times 10^{-5}\ \mathrm{sec}^{-1}$ given by Rees (private communication).

In Fig. 9 we have a plot of our theoretical diffusion coefficient as compared with that of Schunk and Walker (1970). The agreement is never worse than a factor of 2

Fig. 9. A comparison of the computed diffusion coefficient (full line) with those of Schunk and Walker (dashed line) as a function of altitude.

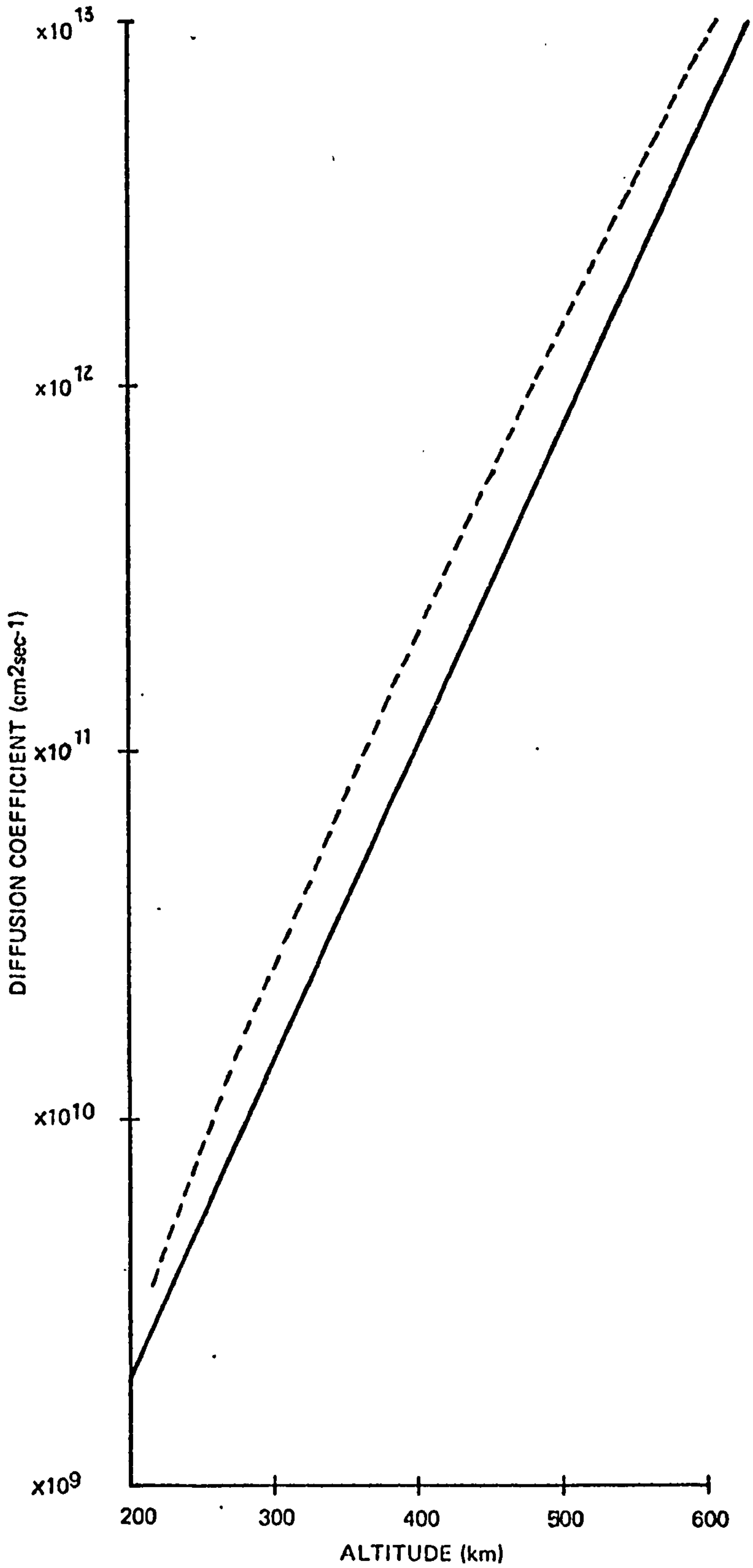
x10^13
x10^12
x10^11
x10^10
x10^9
DIFFUSION COEFFICIENT (cm2sec-1)
200
300
400
500
600
ALTITUDE (km)

from 200 km. up to 600 km. In view of the very large range of diffusion coefficients commonly in use, the agreement must be considered as close. The slope for the diffusion coefficient curve, plotted on a log scale, is controlled by the scale height. If a different value of scale height is used, the disagreement would have been quite significant. It is interesting to note that a choice of scale height based entirely on consideration of the rate of increase of fluctuation also produces a curve for the diffusion coefficient in good agreement with the computed values of Schunk and Walker (1970).

In Fig. 10, we show the theoretical and the experimental electron density profiles. The theoretical profile has been obtained from considerations of the rate of increase of fluctuations as one moves away from the peak position. The experimental profile which is not published has subsequently been made available to us.

Fig. 10. A plot of the deduced electron density profile (full line) against the observed profile (dashed line) as a function of altitude at 1500 hours A.S.T.

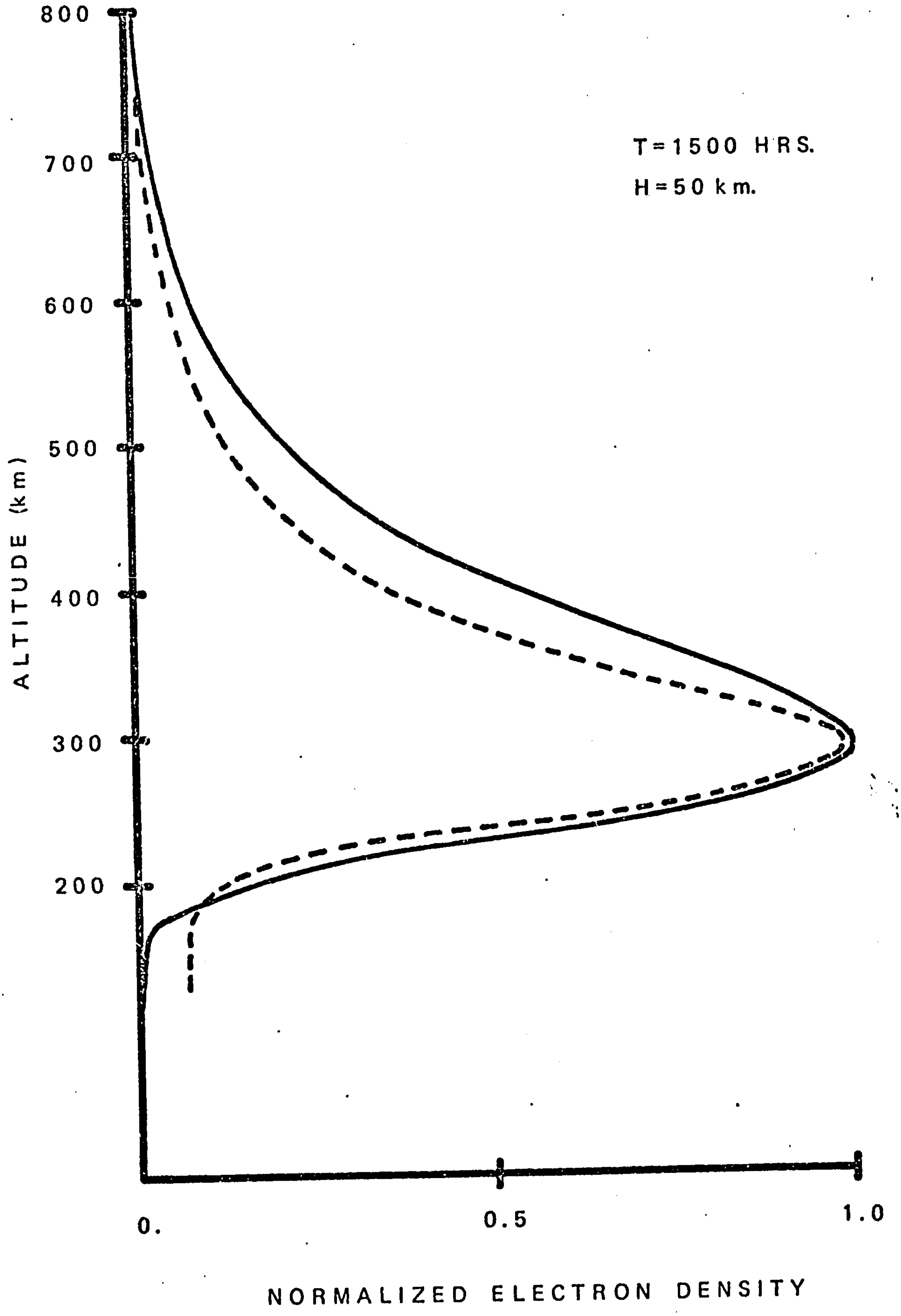
T = 1500 HRS.
H = 50 km.
800
700
600
500
400
300
200
ALTITUDE (km)
0.
0.5
1.0
NORMALIZED ELECTRON DENSITY

Chapter 5

Gravity Wave Induced Behavior in the 6300Å OI and 5200Å NI Airglow Emission

5.1 Theory of 6300Å Airglow Excited Via Dissociative Recombination

As has been pointed out in Chapter 2., dissociative recombination

$$O_2^+ + e \longrightarrow O + O + 6.96 \text{ ev.} \qquad \alpha_1 \qquad (5\text{-}1)$$

$$NO^+ + e \longrightarrow N + O + 2.76 \text{ ev.} \qquad \alpha_2 \qquad (5\text{-}2)$$

may result in the excitation of atomic oxygen or atomic nitrogen levels. We will restrict the development to night-time conditions when reactions (5-1) and (5-2) are the major source of airglow emissions for the 6300Å OI and 5200Å NI lines. The relevant part of the energy level diagrams for both atomic oxygen and atomic nitrogen is shown in Fig. 11. It can be seen that reaction (5-1) is energetically capable of exciting atomic oxygen to the following pairs of terms: (^3P, ^3P), (^3P, ^1S), (^1D, ^1D), or (^1D, ^1S). In the same way reaction (5-2) can produce either the N(^4S) and O(^1D) terms, or the N(^2D) and S(^3P) term.

While we see that reaction (5-1) is capable of exciting the ^1S term of atomic oxygen, other mechanisms of comparable importance not related to F-layer processes also produce

Fig. 11. Energy level diagrams for OI and NI.

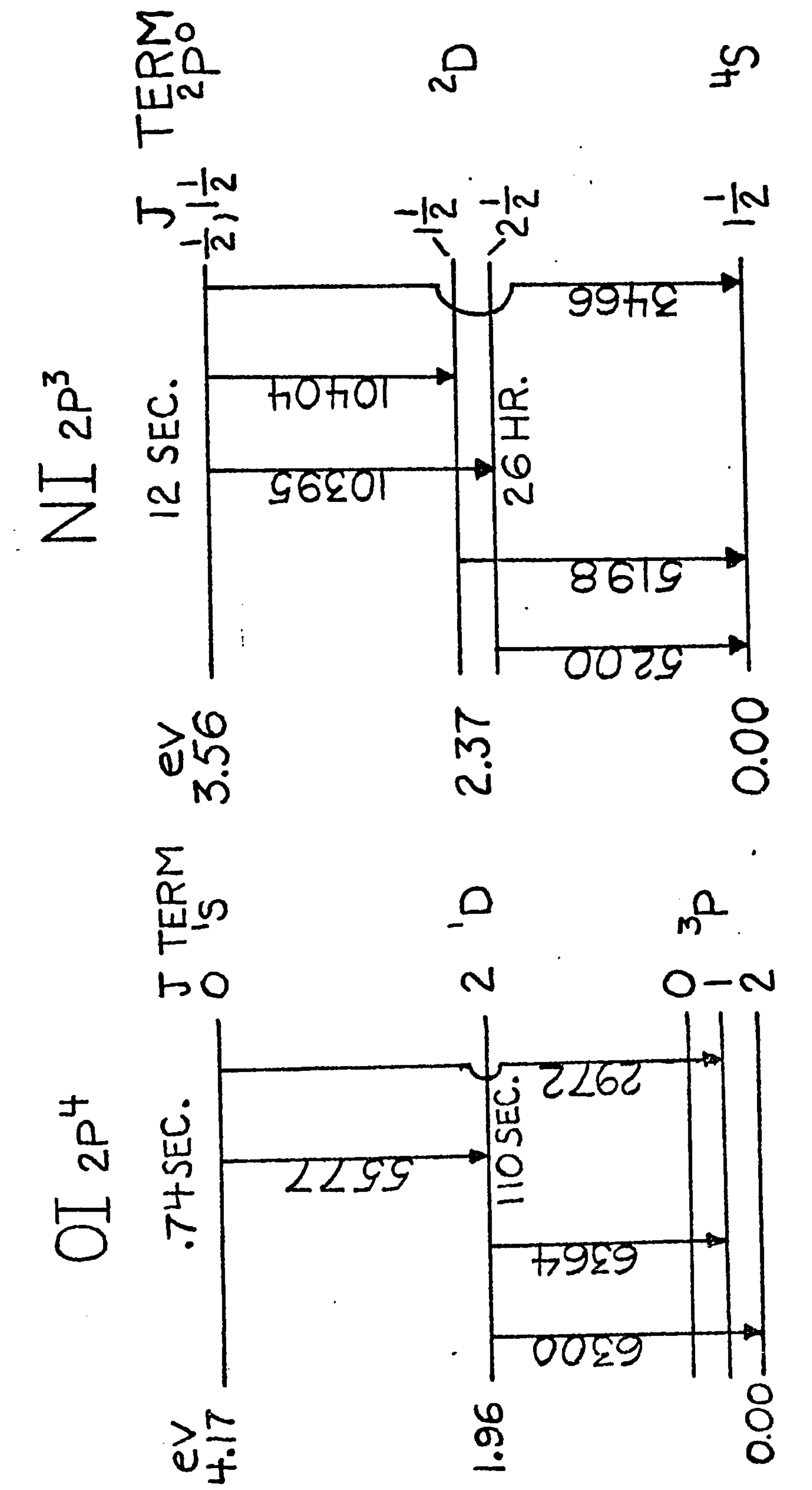
NI 2P^3
ev
3.56
2.37
0.00
J
TERM
^{2}P^o
^{2}D
^{4}S
12 SEC.
26 HR.
10404
10395
34466
5198
5200
OI 2P^4
eV
4.17
1.96
0.00
J TERM
0 ^{1}S
2 ^{1}D
0 1 2 ^{3}P
.74 SEC.
110 SEC.
5577
2972
6364
6300

this excitation. For this reason the 5577Å oxygen green line is a special case and will not be considered further.

The volume emission rate ϵ_λ of a line of wavelength λ from level j is given by

$$\epsilon_\lambda = A_\lambda [j] \tag{5-3}$$

where A_λ is the Einstein transition coefficient for the line of wavelength λ, and $[j]$ is the concentration of atoms in the level j. (The airglow layer is optically very thin, so we may ignore induced transitions.)

The continuity equation for the concentration of atoms in the j^{th} level can be written

$$\frac{\partial [j]}{\partial t} = P_j - L_j \tag{5-4}$$

where P_j is the production rate of atoms in the level j and L_j their loss rate. We have neglected the divergence term since an excited oxygen atom will diffuse only a small distance during its lifetime. (Peterson et. al., 1966)

Production of atoms in the ^1D level can arrise by two processes: Cascade from the ^1S level, and excitation through dissociative recombination from reactions (5-1) and (5-2). However, reaction (5-1) is favored as the primary mechanism (Silverman, 1970). Actual excitation of the ^1S term by reaction (5-1) has been observed to be small (Rishbeth and

Garriott, 1969); hence, we may write the production of $O(^1D)$

$$P_{^1D} = k_{^1D}\alpha_1[O_2^+]N_e \quad (5\text{-}5)$$

where $k_{^1D}$ is the number of excitations of the ^1D level produced per recombination. It is clear from reaction (5-1) that $0 \leq k_{^1D} \leq 2$.

The loss of atoms in the ^1D level occurs both by radiative transition and quenching. The quenching of $O(^1D)$ occurs principally through resonance collisions with O_2 and N_2. N_2 is currently felt to be the dominant quenching agent (Peterson and Van Zandt, 1969). Quenching by super elastic collisions between electons and $O(^1D)$ may also be important in a limited region near the F-layer peak (Brown and Steiger, 1972). The principal reactions may be written

$$O^* \longrightarrow O + h\nu \qquad A_{^1D} \qquad (5\text{-}6)$$

$$O^* + N_2 \longrightarrow N_2^* + O \qquad S_1 \qquad (5\text{-}7)$$

$$O^* + e \longrightarrow O + e \qquad S_2 \qquad (5\text{-}8)$$

Table II gives the magnitude of the rate coefficients.

TABLE II

RATE COEFFICIENTS

Coefficient	Magnitude	Reference
A_{1D}	$1/110\ sec^{-1}$	Chamberlain (1961)
S_1	$5.0 \times 10^{-11} cm^3\ sec^{-1}$	Peterson and Van Zandt (1969)
S_2	$1.7 \times 10^{-9}\ cm^3\ sec^{-1}$	Seaton (1955)

With these considerations the loss of $O(^1D)$ may be written

$$L_{^1D} = \left(A_{^1D} + S_1[N_2] + S_2 N_e\right)[O(^1D)] \qquad (5\text{-}9)$$

where $A_{^1D}$ is the total Einstein transition coefficient from the ^1D level, and S_1 and S_2 are the rate coefficients for quenching with N_2 and N_e respectively.

Using an argument similar to that used in section 2.3 we may neglect the time derivative in equation (5-4) provided the production of $O(^1D)$ does not vary appreciably in the characteristic time $1/\left(A_{^1D} + S_1[N_2] + S_2 N_e\right)$.
It can be seen that this characteristic time is never greater than $1/A_{^1D} = 110$ sec. This time is small compared to gravity wave associated changes occuring in the production term which are of the order of an hour or more.

Setting $\partial[O(^1D)]/\partial t = 0$ we obtain,

$$\epsilon_{63} = \frac{A_{63}}{A_{1D}} \cdot \frac{k_{1D}\, \gamma_1 [O_2]\, N_e}{\left(1 + \frac{S_1[N_2] + S_2 N_e}{A_{1D}}\right)} \qquad (5\text{-}10)$$

where A_{63} is the Einstein transition coefficient for the 6300Å line, and we have replaced $\alpha_1[O_2^+]$ by $\gamma_1[O_2]$, by using results of section 2.3.

In the absence of quenching ($S_1 = S_2 = 0$) we see that equation (5-10) is just proportional to the loss term for the electron density. We recall that $[O_2]$ behaves like e $-Pz/H$; thus, the altitude of the peak volume emission occurs below the altitude of the peak electron density. Since large percentage fluctuations of the electron density occur in this region we expect to see large fluctuations in the peak volume emission. If we now add the quenching term we find that its effect is to increase the altitude at which the peak volume emission occurs since the term $S_1[N_2]$ increases with decreasing altitude. (The electron quenching rate for the 6300Å OI line is always rather small in comparison with the N_2 quenching rate and the radiative transition rate.) Thus, the larger the quenching rate, the higher in altitude the peak volume emission would occur relative to the peak electron density. Since the electron density fluctuations decrease with increasing altitude (provided we remain below the phase change point), a higher altitude in the peak of the volume emission profile implies a decrease in the fluctuation of the magnitude of the peak value.

This situation is not quite this simple, however, since we know from Chapter 3, that the primary effect of the gravity wave is to translate the electrons up and down the magnetic field lines rather than cause an increase or decrease in the total electron content. The combined effect of the exponential behavior of $[O_2]$ and the quenching denominator is to severely restrict the altitude variations of the peak in the volume emission profile. If the peak were to be held fixed at a given altitude its time behavior would be identical to the behavior of the electron density at that same altitude (Fig. 3 and Fig. 4). Thus, if the peak volume emission occurs at an altitude below the electron density peak, we would expect to see rather large fluctuations in the magnitude of the peak volume emission. We will return to this point in section 5.2.

To obtain the zenith airglow intensity from equation (5-10) we integrate over the entire column of atmosphere.

$$I_{63} = \int \epsilon_{63}\, dz = \frac{A_{63}}{A_{1D}} \cdot k_{1D}\gamma_1 \int \frac{[O_2]N_e}{\left(1 + \frac{S_1[N_2] + S_2 N_e}{A_{1D}}\right)}\, dz \quad (5\text{-}11)$$

We see from equation (5-11) that although the peak volume emission may have large percentage fluctuations in magnitude, the 6300Å OI zenith intensity is an integrated effect and need not necessarily show large fluctuation. This can occur both because of the variation of the phase (Fig. 7) and the amplitude of oscillation (Fig. 6) with altitude.

For completeness, we point out that the concentration of O_2^+ is not experimentally observed to increase monotonically with decreasing altitude as would be expected if it were proportional to the concentration of O_2. This inconsistency results from neglecting the concentration of O_2^+ in the equation of charge neutrality. The concentration of O_2^+ becomes comparable to the concentration of O^+ at approximately 170 km. At about 150 km. the concentration of O_2^+ peaks and then begins to decrease with decreasing altitude. Thus it is seen that the approximation of $[O_2^+]$ by $\frac{\gamma_1}{\alpha_1}[O_2]$ overestimates the recombination rate below about 150 km. This has relatively little effect on the behavior of the electron density because we are primarily concerned with altitudes above 200 km. However, since the altitude of the peak volume emission occurs approximately one scale height below the F-layer peak, there is a non-vanishing, although relatively small, contribution to the volume emission profile and, hence to the integrated zenith intensity from altitudes below 170 km.

5.2 Results of Gravity Wave Induced Behavior in 6300A Airglow Emission

In this section we present results obtained using equations (5-10) and (5-11). For consistency we have assumed that $[N_2]_h = [N_2]_{h_0} \exp[-P(h-h_0)/H]$ where $[N_2]_{h_0}$ is obtained from Jacchia's (1964) model atmosphere, and P and H are obtained from the gravity wave results.

We show in Fig. 12 a comparison of the electron density and 6300Å OI volume emission profiles at three different times. The initial values of the peak electron density and the peak luminosity have been normalized to unity at t = 15 00. The gravity wave parameters used here in computing the electron density are the same as those used to fit Thome's results. We have used the values of the quenching coefficients given in Table II.

There are several interesting features here. We note that there is considerable variation in the altitude of the peak electron density, about 50 km., while the variation in the altitude of the peak volume emission is only about 15 km. This small variation of altitude has been explained in section 5.1. Comparing the results at t = 17 3 0 and t = 18 4 5, we note that the magnitude of the peak electron density has decreased due to the general decay of the F-layer. At the same time, however, there is an actual increase of the peak volume emission. This occurrence is a consequence of the entire F-layer moving down in altitude causing an increase in the recombination rate and, hence, in the 6300Å OI volume

Fig. 12. Electron density profiles (upper broader curves) and 6300Å OI volume emission profiles (lower more narrow curves) at three different times. The parameters are the same as used in the fit to Thome's results.

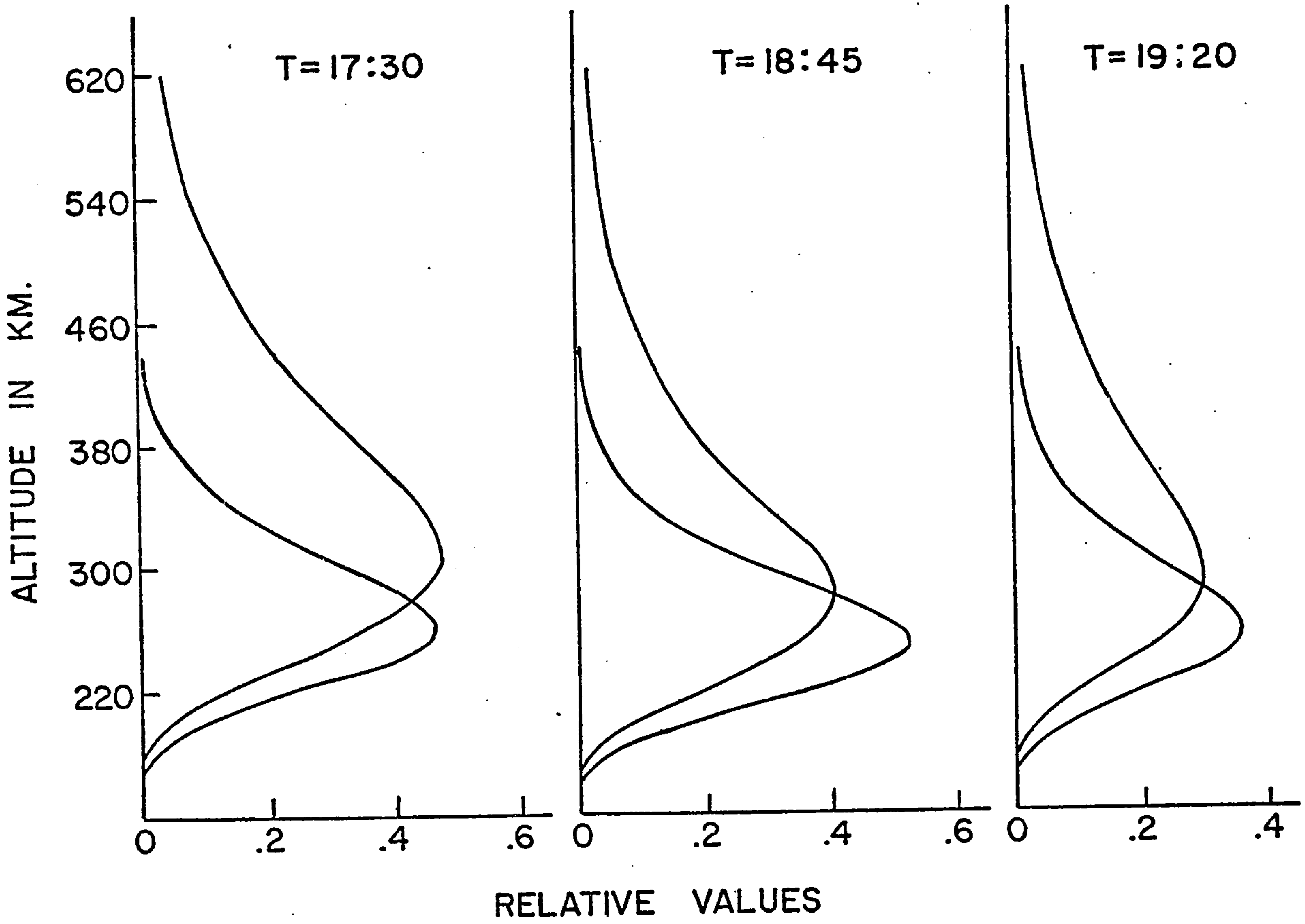
T=17:30
T=18:45
T=19:20
ALTITUDE IN KM.
620
540
460
380
300
220
0
.2
.4
.6
0
.2
.4
.6
0
.2
.4
RELATIVE VALUES

emission. At $t = 1920$ the altitude of the electron density peak is moving up. We note that both the peak electron density and the peak volume emission are decaying. The peak volume emission has decreased markedly. Thus we see, as expected, that the peak value of the volume emission does fluctuate strongly. We should mention that the peak volume emission for the unquenched case occurs at an altitude somewhat below that for the case including quenching and shows a corresponding increase in fluctuation. This is also in agreement with the statements made in section 5.1.

In Fig. 13 we have a comparison of the total columnar electron content, the time rate of change of the total columnar electron content, and the total zenith airglow intensity. We observe that the total columnar electron content shows only weak fluctuation while its time rate of change shows considerable fluctuation. We should point out that if we integrate equation (2-6) over all Z (the flux vanishes at both ends of the atmosphere), we obtain the result that the negative of the time rate of change of total columnar electron content is proportional to the airglow intensity in the absence of quenching. We have seen that the result of an increase in the quenching rate is to translate the entire volume emission profile to higher altitudes and, hence, decrease the fluctuation amplitude of the integrated airglow intensity. (For reasonable values of the parameters appearing in equation (5-10) the altitude of the peak volume

Fig. 13. Time variations of the electron content (—— - —— - ——), the negative of the time rate of change of the electron content (- - - - - - - - -), and the 6300Å OI zenith airglow intensity (full line) using the same parameters as in Fig. 12.

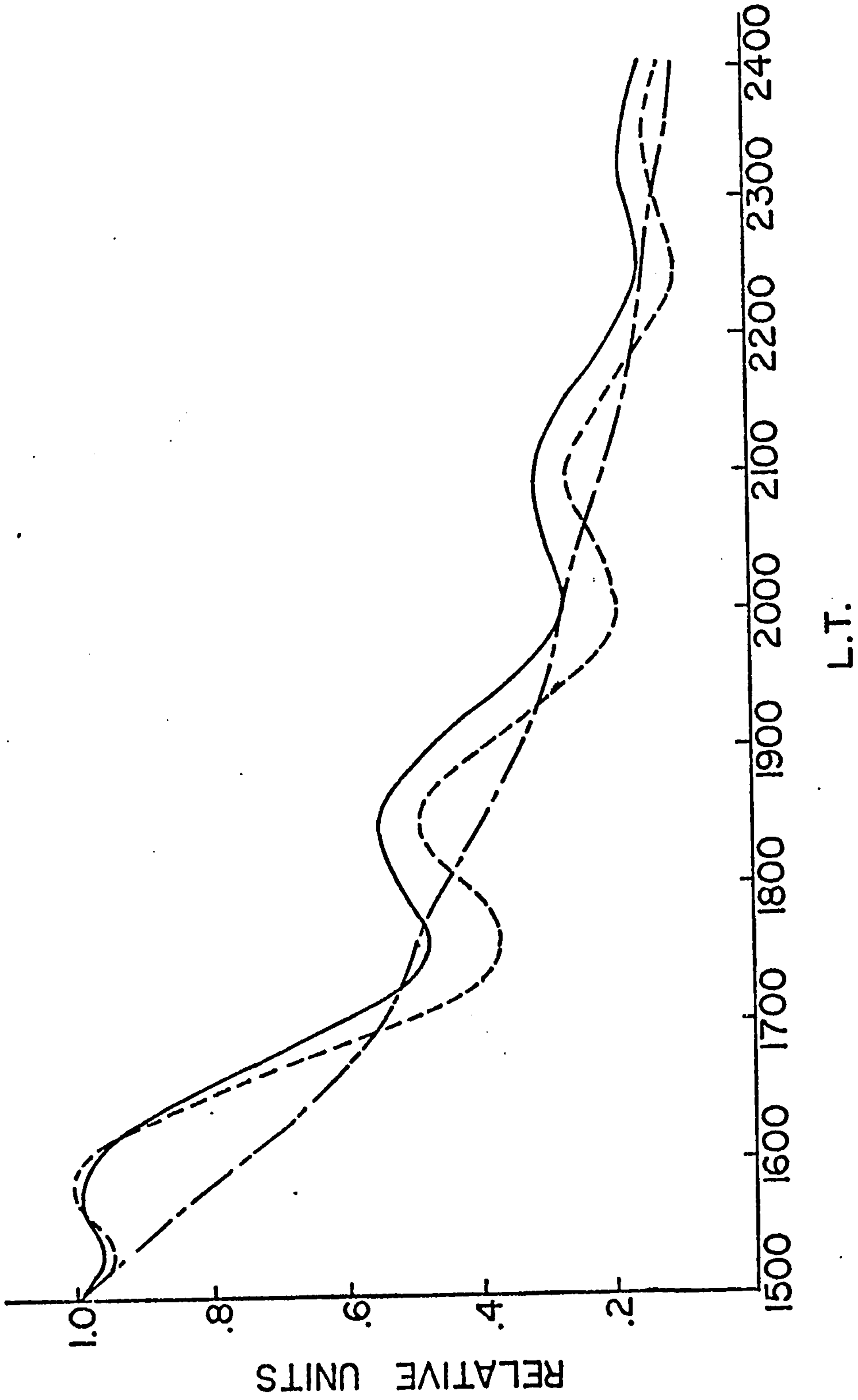
RELATIVE UNITS
1.0
.8
.6
.4
.2
L.T.
1500
1600
1700
1800
1900
2000
2100
2200
2300
2400

emission must remain below the altitude of the peak electron density and in a region where a translation upward in altitude results in a decrease of fluctuation.) Thus, the time rate of change of the total columnar electron content, in general, sets an upper limit for the maximum observable fluctuation in the airglow intensity. We note that, using the quenching coefficients appearing in Table II, the 6300Å OI airglow intensity fluctuations are somewhat reduced relative to the unquenched case but still of the order of 15%.

An interesting result we obtain from this analysis is that the effect of the gravity wave is to essentially move the electrons up and down the magnetic field lines. In which case, the total columnar electron content must always monotonically decrease in the absence of ion pair production mechanisms. If ion pair production occurs, the total columnar electron content would be expected to increase substantially as evidenced by the measurements of Brown and Stieger (1972). Thus, measurements of the total columnar electron content made simultaneously with airglow intensity measurements can be used to distinguish airglow fluctuations produced by waves from those produced by a quasi-periodic ion pair production mechanisms.

We show in Fig. 14 a comparison between experimental measurements of $h'F2$, f_oF2 and the zenith airglow intensity measurements made by Dachs (1968) together with our theoretical fit to his data. We have used the values $p=1.5$,

Fig. 14. Comparison of Dachs' (1968) experimental results (circles) and our theoretical fit (full line), for time variations in $h'F_2$ (upper diagram), f_oF_2 (middle diagram), and 6300Å OI airglow intensity (lower diagram).

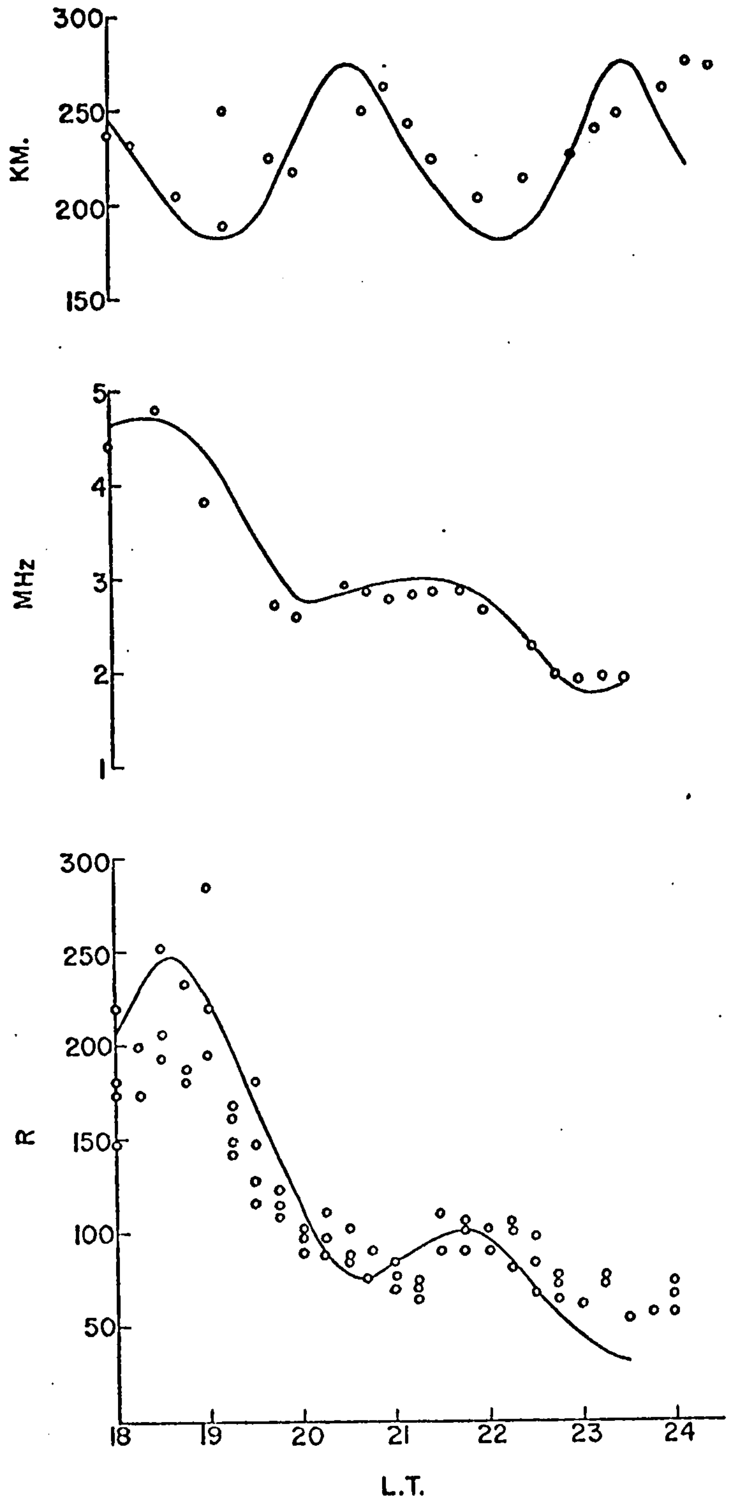

300
250
200
150
KM.
5
4
3
2
1
MHz
300
250
200
150
100
50
R
18
19
20
21
22
23
24
L.T.

$h_0 = 200\,km$, $\alpha = 1.15$, $\beta(h_0) = .34\,Hr^{-1}$, $D(h_0) = 6.1 \times 10^3\,km^2 Hr^{-1}$ and a scale height of 65 km. For the neutral wave we chose $A(h_0) = 35.2$ m sec^{-1} and $q = 0.49$. Based on Jacchia's model atmosphere the quenching rate at h_0 is equal to 0.24 sec^{-1} and quantum efficienty is equal to 0.5.

This experiment is particularly useful because the measurements for the separate quantities are taken simultaneously. Since the theoretical solution is only approximate, we may only compare the general features. We see that the over all phase relationships between the various experimental and theoretical curves are in reasonably good agreement. For example, we see in Dachs' results that when the F-layer peak reaches its maximum altitude the airglow intensity reaches a minimum. The theory shows the same behavior.

In Fig. 15 we show a comparison of the airglow intensities for two different N_2 quenching rates. We are using the same gravity wave parameters as in the comparison with Dachs' results. It can be seen that the large quenching coefficient produces, as expected, smaller oscillation. However, it can also be seen that in addition to the smaller oscillation, a phase advance also arrises. This phase advance is interesting in its own right and occurs principally because, as the quenching coefficient is increased the entire

Fig. 15. Comparison of the time behavior of the 6300Å OI airglow intensity fluctuations for two different quenching coefficients using same parameters as used to fit Dachs' (1968) results. $S_1 = 1.0 \times 10^{-11}$ cm^3 sec^{-1} (full line), $S_1 = 2.7 \times 10^{-10}$ cm^3 sec^{-1} (- - - - -).

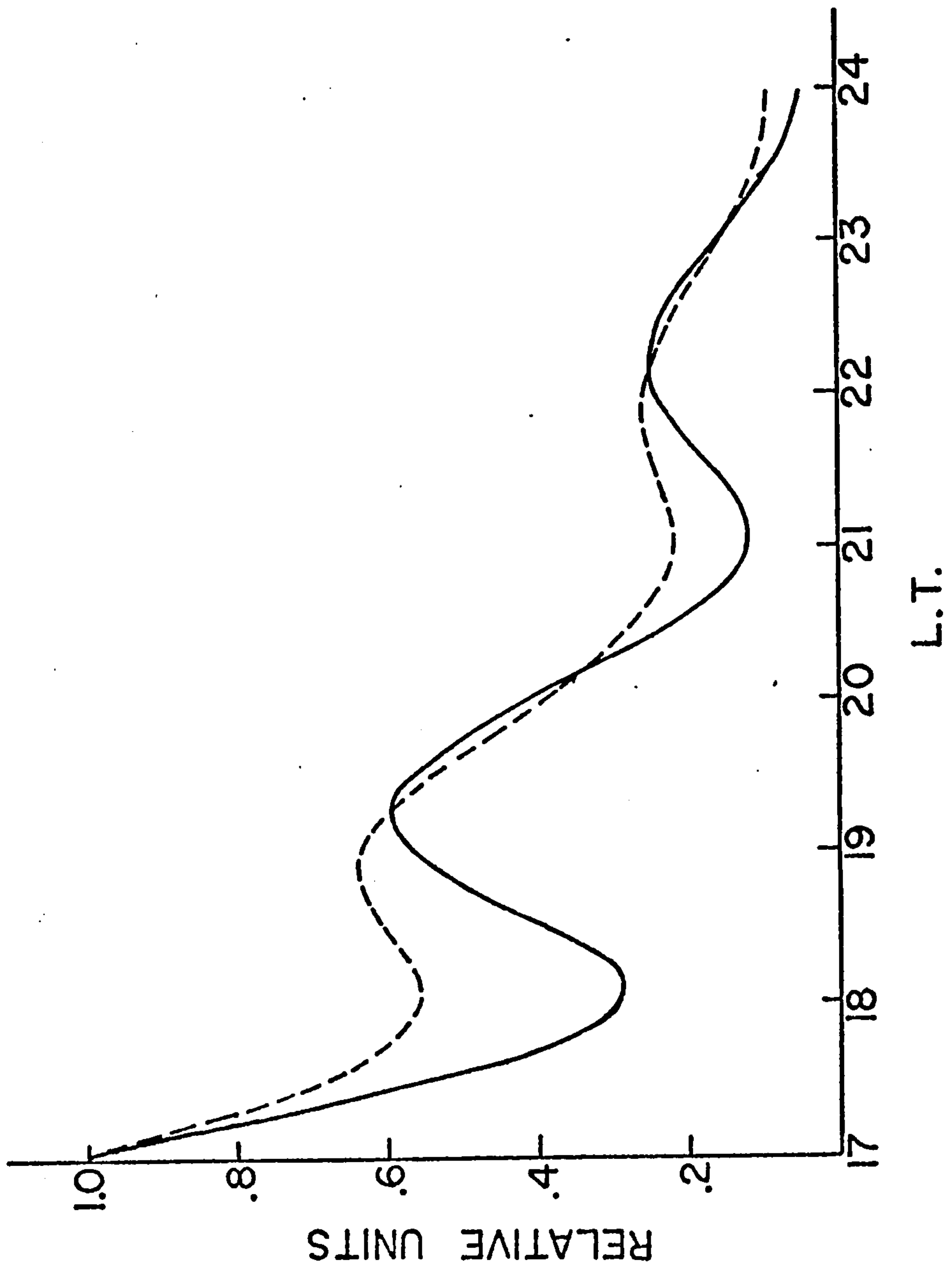
RELATIVE UNITS
1.0
.8
.6
.4
.2
17
18
19
20
21
22
23
24
L.T.

volume emission profile is shifted upward. From our F-layer theory, the electron density oscillations show a monotonic phase advance (Fig. 7) with increasing altitude. Thus if the entire volume emission profile is shifted upward the integrated airglow intensity fluctuations should also show a phase advance. The degree of the phase advance is determined by the shape of the phase variation where the altitude changes occur. For example, we note that in Fig. 13 there is little phase advance observed when comparing the quenched and the unquenched result. This is consistent with the phase diagram in Fig. 7 since the altitude of the peak volume emission is never higher than 250 km. even when quenching is included.

5.3 <u>5200Å NI Theoretical Development</u>

Since the lifetime of 5200Å NI is relatively long, 26 hours (Garstang, 1956), we are forced to use a slightly different development than that used for 6300Å OI. Actually, however, due to collisional de-excitation, the effective lifetime is greatly reduced from 26 hours to, of the order of 25 minutes (Hernandez and Turtle, 1969).

As we have seen in section 5.1, reaction (5-2) may excite the $N(^2D)$ term and it is felt to be the dominant production mechanism. Dissociative recombination of $N_2^+ + e \longrightarrow N + N$ may also excite the $N(^2D)$ term, however, N_2^+ concentrations are extremely small at night (Holmes et.

al., 1965). With these considerations the production term may be written

$$P_{^2D} = k_{^2D} \alpha_2 [NO^+] N_e \tag{5-12}$$

where $K_{^2D}$ is the number of excitations of the ^2D level produced per recombination, clearly $0 \leq k_{^2D} \leq 1$.

The loss of atoms in the ^2D level occurs via the three processes: radiative transition, resonance collisions with O_2, and super elastic collisions with electrons. Super elastic quenching is felt to be important for the $N(^2D)$ term principally because of its long lifetime (Wallace and McElroy, 1966). However, the quenching by O_2 is currently felt to be dominant below about 250 km. (Slanger et. al., 1971). The important reactions are

$$N^* \longrightarrow N + h\nu \qquad A_{^2D} \tag{5-13}$$

$$N^* + O_2 \longrightarrow O_2^* + N \qquad S_3 \tag{5-14}$$

$$N^* + e \longrightarrow N + e \qquad S_4 \tag{5-15}$$

Table III gives the magnitudes of the rate coefficients.

TABLE III

RATE COEFFICIENTS

Coefficient	Rate	Reference
$A_{^2D}$	$1/26\ hr^{-1}$	Garstang (1956)
S_3	$1.4 \times 10^{-12} cm^3 sec^{-1}$	Hernandez and Turtle (1969)
	$1.6 \times 10^{-11} cm^3 sec^{-1}$	Slanger et.al. (1971)
S_4	$8 \times 10^{-10}\ cm^3 sec^{-1}$	Seaton (1956)

With these considerations, we may write the loss of $N(^2D)$ as

$$L_{^2D} = \left(A_{^2D} + S_3[O_2] + S_4 N_e\right)\left[N(^2D)\right] \tag{5-16}$$

where $A_{^2D}$ is the total Einstein radiative transition coefficient from the ^2D term, and S_3 and S_4 are the rate coefficients for quenching with O_2 and N_e respectively. Letting

$$Q = \frac{S_3[N_2] + S_4 N_e}{A_{^2D}}$$

$$L_{^2D} = A_{^2D}(1+Q)\left[N(^2D)\right] \tag{5-17}$$

The continuity equation for $\left[N(^2D)\right]$ may be written

$$\frac{\partial\left[N(^2D)\right]}{\partial t} = P_{^2D} - A_{^2D}(1+Q)\left[N(^2D)\right] \tag{5-18}$$

where we have neglected the divergence term on the basis that an excited $N(^2D)$ atom will diffuse only a short distance during its effective lifetime (Hernandez and Turtle, 1969). It is clear that we can not assume quasistatic equilibrium, in general, for equation (5-18), since the characteristic time over which the production term must be slowly varying is as large as $1/A_{^2D}$ = 26 hours. Exact time dependent solution for this equation is given by

$$[N(^2D)]_t = [N(^2D)]_{t_0} \exp\left[\int_{t_0}^{t} -A_{^2D}(1+Q)\,dt'\right] + \exp\left[-A_{^2D}\int_{t_0}^{t}(1+Q)\,dt'\right]\int_{t_0}^{t}\left[P_{^2D}(t')\exp\left(A_{^2D}\int_{t_0}^{t'}(1+Q)\,dt''\right)\right]dt' \quad (5\text{-}19)$$

The volume emission is

$$\epsilon_{52} = A_{52}[N(^2D)]_t \quad (5\text{-}20)$$

We see that in the long time limit ($t \gg t_o$) and when $P_{^2D}$ and $L_{^2D}$ are constant in time, then equation (5-20) reduces to the same form as equation (5-10).

The zenith intensity for 5200Å NI can be written

$$I_{52} = \int \epsilon_{52}\, dz \quad (5\text{-}21)$$

where the integration is taken over the entire column of atmosphere.

5.4 Results of the 5200Å NI Airglow

Numerical methods are used to integrate expression (5-19) and (5-21). Results of these integrations are shown in Fig. 16. The gravity wave parameters are the same as those used to fit Thome's results. We observe that there is a decrease in the fluctuation amplitude and a phase advance associated with the higher quenching rate. Both of these features may be explained in the same manner as before.

An interesting property of the 5200Å line is that the fluctuation amplitude of the airglow intensity is very sensitive to the quenching rate of O_2 and relative to the electron quenching rate. This is a consequence of several factors. The O_2 quenching rate of the $N(^2D)$ term is reduced considerably relative to N_2 quenching of the $O(^1D)$ term. This occurs both because the rate coefficient is smaller and because the abundance of O_2 at a given altitude is small relative to N_2. At the same time the electron quenching rate of the $N(^2D)$ term is large over an extended altitude range both because of the lower O_2 quenching rate and the long radiative lifetime of the $N(^2D)$ term.

It is interesting to note that increasing the electron quenching rate relative to the O_2 quenching rate produces an increase in the fluctuation amplitude of the airglow intensity. This occurs because the electron density increases with altitude below the F-layer peak and therefore has the effect of pushing the altitude of the peak volume emission

Fig. 16. Comparison of the time behavior of the 5200Å NI airglow intensity fluctuations for quenching coefficients used by Hernandez and Turtle (1969) (- - - - -), and those used for the 6300Å line in Fig. 12 (full line).

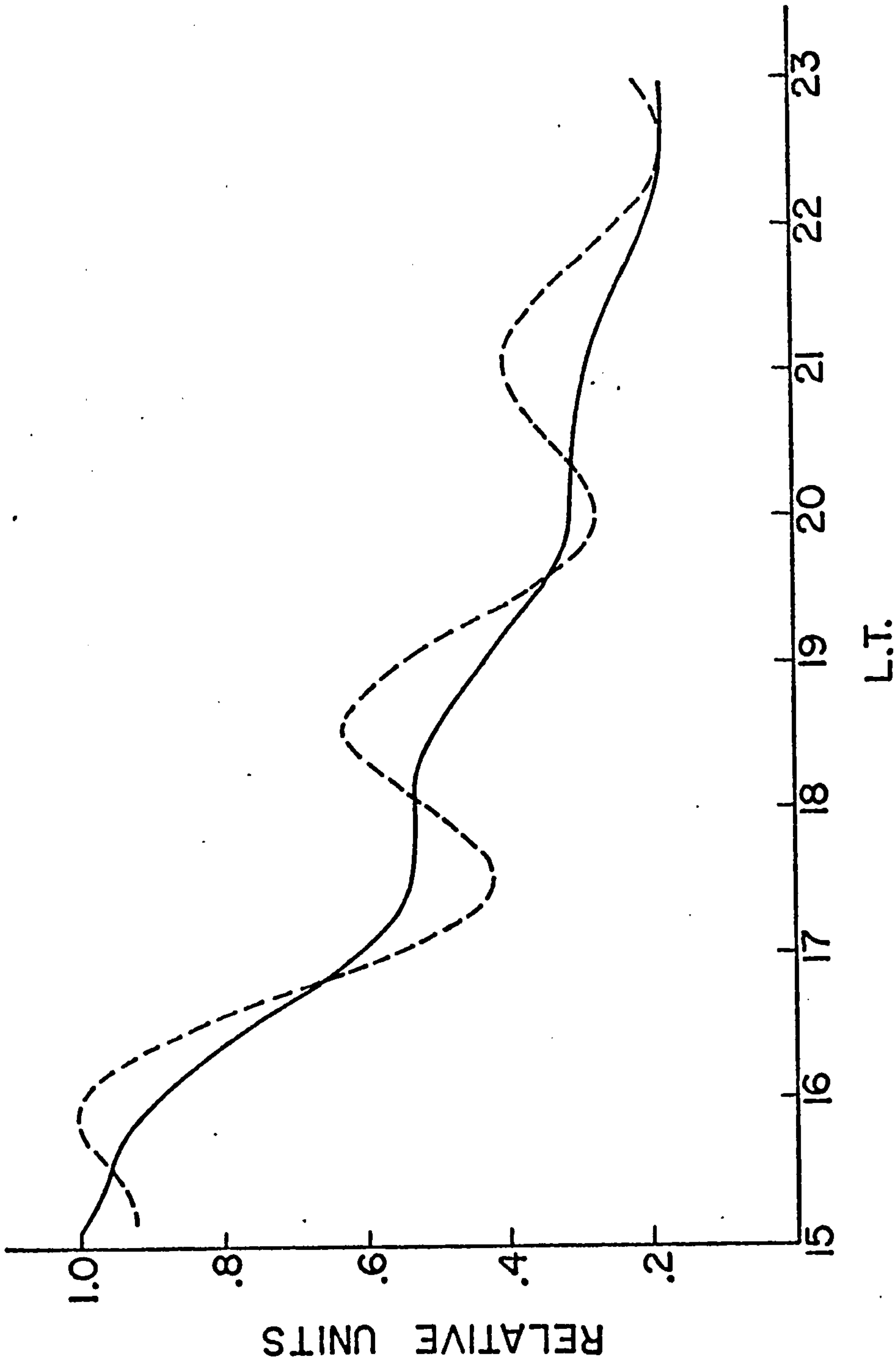
RELATIVE UNITS
1.0
.8
.6
.4
.2
15
16
17
18
19
20
21
22
23
L.T.

lower as the electron quenching rate is increased. (This effect would also occur in the 6300Å line except that the radiative transition rate is always large compared to the electron quenching.) Since the amplitude of the oscillation of the airglow intensity depends strongly on the altitude at which the peak volume emission occurs, experimental measurements of the 5200Å airglow intensity fluctuations would give an indication of the quenching rate for O_2 relative to that for electrons. We note that there is still some uncertainty in the magnitude of the O_2 quenching rate coefficient (Slanger et. al., 1971).

Chapter 6

Conclusion

Using our theoretical formulation we have made a detailed comparison with a careful and detailed experiment. The over all agreement obtained indicates that TID observed at Arecibo by Thome (1968) can be satisfactorally explained in terms of ionospheric response to gravity waves. Our theoretical analysis shows that even for simple sinusoidal ducted gravity wave models the detailed behavior of the F-layer response can be quite complex. This analysis suggests that long period, long wavelength waves are not appreciably damped with altitude, as evidenced by the unattenuated fluctuations observed by Thome (1968) even for altitudes well above 500 km. It is found that the fluctuations in the electron density at about two scale heights below the peak are typically 6 to 8 times the fluctuations at the peak, and are comparable to the average unperturbed electron density. Consequently, our method has definite advantage over a strict perturbation approach used in most theoretical treatments, since the latter can no longer apply at these altitudes. It is of interest to note that the downward phase progression observed in the vertical structure of TID can be explained in terms of the shape of the electron density profile without requiring a vertical downward phase progression in the neutral wave. This is demonstrated clearly by our theoretical results where the F-layer response shows a monotonic phase advance with increasing altitude even though the gravity wave is assumed to be fully ducted with no vertical phase progression.

In comparison to the large altitude variations found for the peak electron density during the passage of a gravity wave, the altitude of the peak volume emission is found to be greatly restricted in its oscillations. For this reason, the time dependent behavior of the peak volume emission is similar to that of the electron density oscillation at constant altitude. As a consequence, the amplitude and phase of the airglow intensity fluctuation depend strongly on the quenching rate. The fluctuation amplitude for the 5200Å NI airglow intensity is found to be sensitive to the relative quenching of $N(^2D)$ by electrons as compared to O_2.

APPENDIX A

Since all of our solutions are expressed in terms of linear combinations of Chapman's function, we need only to show that the variations in a simple Chapman solution caused by small variations in β and D_a are unimportant except at altitudes well below the electron density peak. Our argument is similar to Hooke's (1968) argument concerning variations in the photoionization rate during passage of a gravity wave.

For a simple Chapman solution we may write

$$\frac{N_e(\beta+\delta\beta)-N_e(\beta)}{N_e(\beta)} = \left[\left(1+\frac{\delta\beta}{4\beta}\right)e^{-\frac{\alpha}{4}\frac{\delta\beta}{\beta}e^{-\frac{z}{H}}} - 1\right]$$

$$= \left[\left(1+\frac{\delta\beta}{4\beta}\right)e^{-X\frac{\delta\beta}{4\beta}} - 1\right] \qquad \text{(A-1)}$$

where we have replaced $\alpha e^{-\frac{z}{H}}$ by the dimensionless variable X. For variations of $\delta\beta/\beta = -8\%$ corresponding variations of the electron density remain less than 10%, provided the altitude is not extended lower than approximately three scale heights below the F-layer peak. (For the parameters used in fitting Thome's results this condition requires that we restrict the altitude to be above about 150 km.) A similar argument can be used for neglecting small variations in D_a.

REFERENCES

Akasofu, S. I. 1956. Sci. Repts. Tohoku Univ. Geophys. 8, 24.

Biondi, M. A. 1969. Can. J. Chem. 47, 1711.

Bowman, G. G. 1965. J. Atmos. Terr. Phys. 27, 1247.

Brown, W. E. and Steiger, W. R. 1972. Planet. Space Sci. 20, 11.

Chamberlain, J. W. 1961. Physics of the Aurora and Airglow. Academic Press, New York.

Dachs, J. 1968. Beitr. Phys. Atm. 41, 184.

Donahue, T. M. 1968. Science, N.Y. 159, 489.

Dungey, J. W. 1955. The physics of the ionosphere (The Physical Society, London) p. 229.

Ferraro, V. C. A. 1945. Terr. Mag. 50, 215.

Ferraro, V. C. A. 1946. Terr. Mag. 51, 427.

Ferraro, V. C. A. and Ozdogan, I. 1958. J. Atmos. Terr. Phys. 12, 140.

Garstang, R. H. 1956. The Airglow and the Aurora. (Ed. E. B. Armstrong and A. Dalgarno), p. 324. Pergamon Press, Oxford.

Glidden, J. E. C. 1959. Quart. J. Mech. Appl. Math. 12, 347.

Hernandez, G. and Turtle, J. P. 1969. Planet Space Sci. 17, 675.

Hooke, W. H. 1968. J. Atmos. Terr. Phys. 30, 795.

Hines, C. O. 1960. Can. J. Phys. 38, 1441.

Holmes, J. C., Johnson, C. Y. and Young, J. M. 1965. Space Res. 5, 756.

Jacchia, L. G. 1965. Smithson. Contr. Astrophys. 8, 215.

Klostermeyer, J. 1972a. J. Atmos. Terr. Phys. 34, 765.

Klostermeyer, J. 1972b. J. Atmos. Terr. Phys. 34, 1393.

Martyn, D. F. 1950 Proc. Roy. Soc. A 201, 216.

Moschandreas, D. J. and Tuan, T. F. 1973. to be published.

Nelson, R. A. 1968. J. Atmos. Terr. Phys. 30, 825.

Peterson, V. L., Van Zandt, T. E. and Norton, R. B. 1966. J. Geophys. Res. 71, 2255.

Peterson, V. L. and Van Zandt, T. E. 1969. Planet. Space Sci. 17, 1725.

Rishbeth, H. and Garriott, O. K. 1969. Introduction to Ionospheric Physics. Academic Press, New York.

Seaton, M. J. 1956. The Airglow and the Aurora. (Ed. E. B. Armstrong and A. Dalgarno), p. 289. Pergamon Press, Oxford.

Schunk, R. W. and Walker, J. C. G. 1970. Planet. Space Sci. 18, 1391.

Silverman, S. M. 1970. Space Sci. Rev. II, 341.

Slanger, T. G., Wood, B. J. and Black, G. 1971. J. Geophys. Res. 76, 8430.

Testud, J. and Francois, P. 1971. J. Atmos. Terr. Phys. 33, 765.

Thome, G. D. 1968. J. Geophys. Res. 73, 6319.

Thome, G. D. 1964. J. Geophys. Res. 69, 4047.

Tuan, T. F. 1968. J. Phys. B. (PROC. Phys. Soc.), (2), 1, 966.

Tuan, T. F. 1969. Astrophys. J. 157, 1449.

Volland, H. 1969a. J. Atmos. Terr. Phys. 31, 491.

Volland, H. 1969b. J. Geophys. Res. 74, 1786.

Wallace, L. and McElroy, M. B. 1966. Planet. Space Sci. 14, 677.